chromatography, other dominant blood cells cause interference (11). In blood purification, the elimination of specific cytokines such as interleukin-1 or tumor necrosis factor, which are the major pathogenic mediators in septic shock and multiorgan failure, has been proposed (12).

Magnetic particles are also used in immunoassays (13, 14). Immunoassays are widely used for medical examinations (*e.g.*, detection of viruses or assay of various hormones) (15, 16). Magnetic separation is a suitable method to reduce the duration of both adsorption and separation steps (17).

Nagatani *et al.* (18) reported a unique approach for transfecting cells using magnetite cationic liposomes (MCLs) associated with a plasmid vector and the selection of transformants using a magnetic field. In clinical applications, somatic cells that are transformed to produce specific proteins should be rapidly selected on account of the limited number of cell divisions. Therefore, the rapid selection of transformants among a transiently transformed population is important. Selection using antibiotic-resistance marker genes is, however, time consuming; furthermore, the recovery of the transformants cannot be guaranteed, because the transformation efficiency depends on the cell line used. When MCLs associated with a plasmid vector were transfected into mouse NIH/3T3 cells, the specific activity of the luciferase gene transfectants was approximately 7-fold higher than that of the cells before separation using the magnetic field. Some researchers have reported the separation of transiently transfected cells using magnetic particles associated with antibodies (19–21). However, this method requires the cotransfection of a gene for the expression of a surface marker. In the method developed by Nagatani *et al.* (18), the expression of an additional marker is not required for separation, and magnetic separation can be performed immediately after transformation. This is a major advantage for the separation of transformants.

II. MAGNETIC RESONANCE IMAGING AND CANCER DIAGNOSIS

The applications of MRI have steadily increased over the past decade. MRI offers the advantage of high spatial resolution of contrast differences between tissues. Due to the unique function of this imaging modality, there is a need to develop effective contrast agents that will enhance and widen its diagnostic utility. Paramagnetic ion chelates and ferromagnetic or superparamagnetic nanoparticles, with sizes that generally range between 3 and 10 nm, have been developed as MR contrast agents and used in clinical diagnosis. In most situations, they are used for their effects, which result in signal reduction on T_2-weighted images ("negative" contrast).

During recent years, there has been an increase in interest regarding the use of magnetic nanoparticles as contrast agents, such as dextran magnetite in MRI (22, 23). In comparison to paramagnetic ions, super-paramagnetic iron oxide particles have higher molar relaxivities, and when used as blood pool and tissue-specific agents, they may offer advantages at low concentrations (24, 25).

Commercial contrast agents do not have active targeting ability, but are useful for enhancing the contrast differences of the liver or spleen because magnetic nanoparticles accumulate in the reticuloendothelial system such as the liver and spleen (passive targeting). Suzuki *et al.* (26) studied the specific distribution of these agents by active targeting. Monoclonal antibodies (MAbs) specifically targeted to cancer cells could serve as a possible tool for active targeting. They developed an MRI contrast agent, MAb-magnetite (Fig. 1A), which was prepared by covalently linking polyethylene glycol-coated magnetite to a MAb specific for a human glioma cell surface antigen. When MAb-magnetite was injected intravenously into tumor-bearing nude mice, magnetite nanoparticles accumulated in the tumor tissue 24 or 48 h after the MAb-magnetite injection, and a 50% decrease in the T_2 signal intensity of the tumor was observed as shown in Fig. 1B (26).

Shinkai *et al.* (27) and Uchiyama *et al.* (28) have proposed a direct sensing method for magnetic nanoparticles in cancer diagnosis. They developed a small and highly sensitive magnetic sensor, the magneto impedance (MI) sensor, for the sensing of tumor tissue that incorporates magnetic particles. They attempted to detect magnetic particles in a rat glioma, a malignant brain tumor, transplanted under the

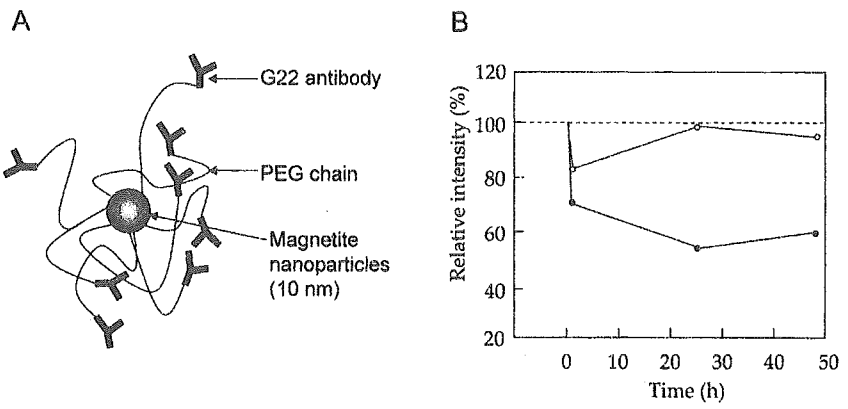

FIG. 1. MAb-magnetite used as an MRI contrast agent. MAb magnetite (A) was prepared by covalently linking polyethylene glycol-coated magnetite to G22 antibody. MAb-magnetite was injected intravenously into subcutaneous glioma-bearing nude mice. MR images were acquired 30 min, 24 h, and 48 h following the administration of MAb-magnetite. (B) Comparison of the intensities of the T_2 signals of the tumor between magnetite nanoparticles with (closed circles) or without (open circles) G22 antibody.

skin of a rat's leg (27). The magnetic nanoparticles in the tumor were magnetized by a static magnetic field generator at 1.8 T. The magnetic field distribution of the magnetic nanoparticles was detected using the MI sensor; furthermore, its distribution indicated that the magnetic nanoparticles were localized only in the tumor. When these apparatuses are available for clinical use, the diagnosis of metastatic cancer with high sensitivity will be possible.

III. MAGNETIC-NANOPARTICLE-INDUCED HYPERTHERMIA

"*Quae medicamenta non sanat; ferrum sanat. Quae ferrum non sanat; ignis sanat. Quae vero ignis non sanat; insanabilia reportari oportet*" — Hippocrates.

(Those diseases which medicines do not cure, the knife cures; those which the knife cannot cure, fire cures; and those which fire cannot cure, are to be reckoned wholly incurable.)

As Hippocrates (460–370 BC) described in his aphorism, he believed that any disease could be cured by heating the patient's body. Hyperthermia is a promising approach to cancer therapy, and various methods inducing hyperthermia, such as the use of hot water, capacitive heating, and induction heating among others, have been employed (29–32). A major technical problem with the application of hyperthermic treatments is the difficulty in heating the local tumor region to the intended temperature without damaging normal tissue. Conventional hyperthermic systems are designed to heat tissue to approximately 42.5°C to 44.0°C. However, higher temperatures can kill a greater number of tumor cells, and in principle, tumor-specific hyperthermia can kill all types of tumor cells.

Some researchers have proposed the concept of "intracellular" hyperthermia and have developed submicron magnetic particles for inducing hyperthermia (33–35). This concept is based on the principle that under an alternating magnetic field (AMF), a magnetic particle can generate heat by hysteresis loss. In 1979, Gordon *et al.* (36) first proposed the concept of inducing intracellular hyperthermia using dextran magnetite nanoparticles. They administered magnetite nanoparticles intravenously to Sprague–Dawley rats bearing mammary carcinomas and showed that AMF-induced heating occurred in their *in vivo* experiments. Jordan *et al.* (37) have proposed magnetic fluid hyperthermia in several other comprehensive *in vitro* studies.

The important properties of magnetic particles for inducing hyperthermia are nontoxicity, biocompatibility, injectability, high-level accumulation in the target tumor and effective absorption of the energy of AMF. Chan *et al.* (38) reported on modified dextran magnetite and its hyperthermic effect by using several human carcinoma cell lines *in vitro*. The specific absorption rate (SAR), which indicates the heat evolution rate in hyperthermia, of conventional dextran magnetite is low. Dextran magnetite behaves as a super-paramagnetic particle rather than a ferromagnetic particle due to its small size; hence, its hysteresis loss is very low. Chan *et al.* (38) controlled the oxygen concentration in the preparation of dextran magnetite and selected particles of approximately 15 nm. Shinkai *et al.* (39) have reported that particle size is a critical factor in obtaining a high SAR value.

IV. HYPERTHERMIA USING MAGNETITE CATIONIC LIPOSOMES

Since the administered particles passively migrate to a reticuloendothelial system such as the Kupffer cells of the liver and spleen, the passive targeting of magnetic nanoparticles for cancer is a very important issue. With regard to the drug delivery of magnetic nanoparticles, magnetoliposomes may be a promising tool for passive targeting. This type of vesicle consists of magnetic nanoparticles wrapped in a phospholipid bilayer (liposome). Liposomes have structural and biokinetic advantages such as their ability to encapsulate therapeutic drugs or genes. Furthermore, the liposomal surface could be chemically modified in order to enable targeting to a specific tissue. Since the localization of vesicles in tumor cells can be enhanced by their surface charge, Shinkai *et al.* (40) developed MCLs (Fig. 2A) with improved adsorption and accumulation properties. As shown in Fig. 2B, MCLs, which have a positive surface charge, showed a 10-fold higher affinity for rat glioma cells as compared to neutrally charged magnetoliposomes. MCLs have a sufficiently high SAR and a general biocompatibility that are comparable to those of dextran magnetite. The Kobayashi research group demonstrated the efficacy of hyperthermia by using MCLs in animals with several types of tumors, such as the B16 mouse melanoma (41), T-9 rat glioma (42), Os515 hamster osteosarcoma (43), and VX-7 squamous cell carcinoma in rabbit tongue (44).

In an experimental model using T-9 rat glioma (42), MCLs were injected into solid tumors formed subcutaneously in F344 rats. Subsequently, the rats were exposed to an AMF for 30 min once (group II), twice (group III), or three times (group IV). In the control group (group I), the rats were administered MCLs but were not exposed to AMF. The temperature of the tumor was rapidly elevated by AMF exposure and it exceeded 43°C after 15 min, as shown in Fig. 2C. In contrast, the rectal temperature or the temperature in a tumor lacking the MCLs remained between 35–37°C. In group II, the decrease in the average tumor volume was not significant. However, in the case of groups III and IV, in which the animals received repeated AMF exposure, the average tumor volume decreased markedly.

Complete regression was observed in one of the five rats in group II, three of the five in group III, and seven of the eight in group IV. This confirmed the effectiveness of multiple AMF exposures in attaining tumor regression. In group IV, only one tumor exhibited no regression. Figure 2D shows the time courses of tumor growth. The tumor volume in control rats (no AMF exposure) steadily increased with no evidence of regression. In contrast, complete tumor regression was observed in many of the rats subjected to three AMF exposures, at 24-h intervals. In most cases of complete regression, the tumor volume increased up to the 12th day, after which it began to decrease and the tumor finally disappeared. No regrowth of tumors was observed following complete regression over a period of 3 months.

To achieve complete tumor regression, multiple AMF exposure is very important. Ito *et al.* (45) showed that com-

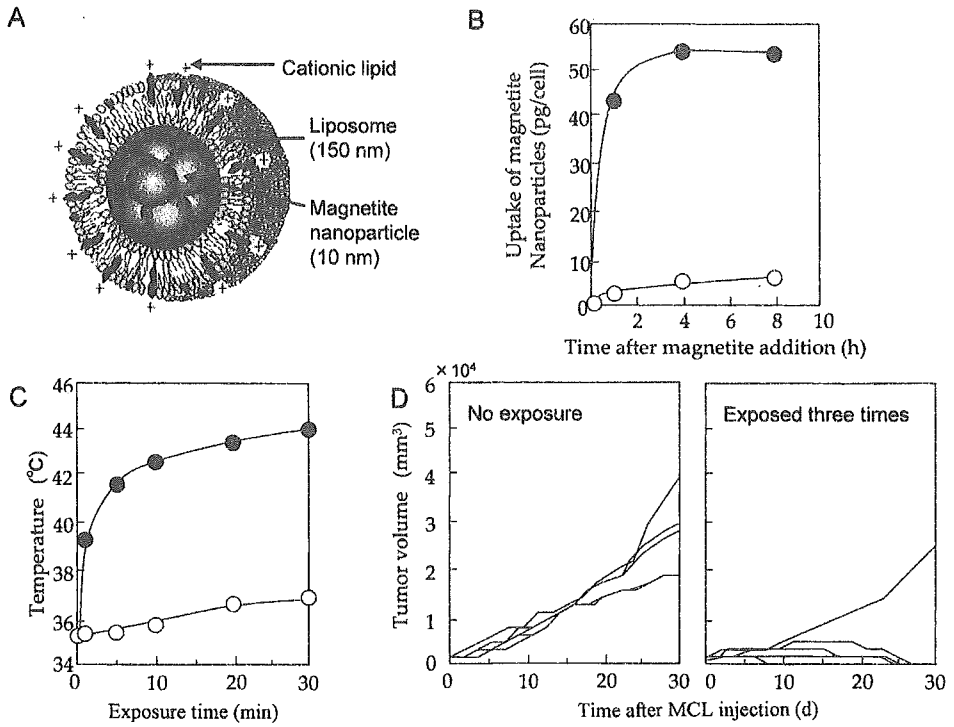

FIG. 2. Magnetite cationic liposomes (MCLs) for hyperthermia. Magnetite nanoparticles were wrapped in cationic liposomes (A). (B) Comparison of magnetite uptake by T-9 rat glioma cells *in vitro* between MCLs (closed circles) and neutrally charged magnetoliposomes (MLs, open circles). For the *in vivo* experiment (C), MCLs were directly injected into a subcutaneous T-9 tumor, and an alternating magnetic field (AMF, 118 kHz and 384 Oe) was applied for 30 min. Temperature increases of the outer covering of the tumor (closed circles) and of the rectum (open circles) during magnetic field irradiation. (D) The time courses of the tumor growth. In nonexposed animals, the tumor volume in each rat steadily increased with no evidence of regression. In contrast, complete tumor regression was observed in 88% of the rats that were exposed three times to the AMF. Tumor regrowth over a 3-month period was not observed following complete regression. Each line represents an individual rat.

plete regression of mammary carcinomas of a size greater than 15 mm by frequent repeated hyperthermic treatments using MCLs was obtained in all mice. In these studies, 40–60% of the injected MCLs accumulated in the tumor tissue, whereas only 20–25% of the neutral magnetoliposomes accumulated. This high accumulation of MCLs is considered to be due to the cationic charge on the surface of the liposome used. Furthermore, a significant hyperthermic effect was achieved.

V. HYPERTHERMIA USING ANTIBODY-CONJUGATED MAGNETITE NANOPARTICLES

Administration of the MCLs is limited to direct injection into the tumor tissue. If magnetic nanoparticles adsorb only to cancer cells, the particles could be administered intravenously. This feature would be of great advantage in terms of the quality of life of patients, and would enable cancer diagnosis by MRI and concurrent hyperthermic treatment (the proposed therapeutic strategy using the magnetic particles is illustrated in Fig. 3). The conjugation of antibodies to magnetic particles is a possible approach to achieving such an aim.

Le *et al.* (46) and Shinkai *et al.* (47) have developed magnetite nanoparticles conjugated to the Fab' fragments of anti-human MN antigen-specific antibody and their hyperthermic effects were demonstrated using a mouse renal cell carcinoma model. Human MN antigen is a cell-surface antigen frequently expressed in clear-cell type renal cell carcinoma, but not detected in normal kidney. The Fab' fragment of the G250 antibody that binds to the MN antigen on many types of human renal cell carcinomas was cross-linked to *N*-(6-maleimidocaproyloxy)-dipalmitoylphosphatidylethanolamine (EMC-DPPE) in the liposomal membrane. The targeting ability of the G250 antibody-conjugated magnetoliposomes (G250-AMLs, Fig. 4A) was investigated using a mouse renal cell carcinoma (mRCC) and MN antigen-presenting cells, MN antigen-overexpressing mouse renal cell carcinoma (MN-mRCC) (47). In an *in vivo* experiment using MN-mRCC-harboring mice, 7.9 mg of the AMLs per gram of carcinoma tissue (the tumor weight: 0.19 g) were found to be accumulated, which corresponded to approximately 50% of the total amount injected (Fig. 4B). After injection of the AMLs, the mice were subjected to AMF exposure. The temperature of the tumor tissue increased to 43°C and the growth of the carcinoma was significantly arrested for at least 2 weeks (Fig. 4C). These results indicate that the G250-AMLs could target the renal cell carcinomas *in vitro* and *in vivo*, and that they are suitable for the efficient hyperthermic treatment of carcinomas.

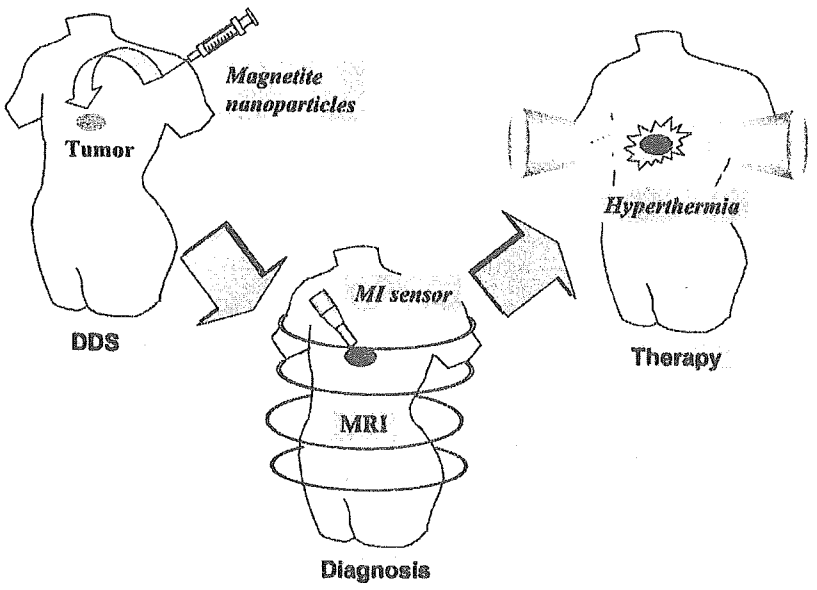

FIG. 3. Schematic illustration of the therapeutic strategy using magnetic particles. Functionalized magnetic nanoparticles accumulate in the tumor tissues via the drug delivery system (DDS). Magnetic nanoparticles can be used as a tool for cancer diagnosis by magnetic resonance imaging (MRI) or for magnetoimpedance (MI) sensor. Hyperthermia can then be induced by AMF exposure. Thus, magnetic nanoparticles can be used for cancer therapy at the same time as diagnosis.

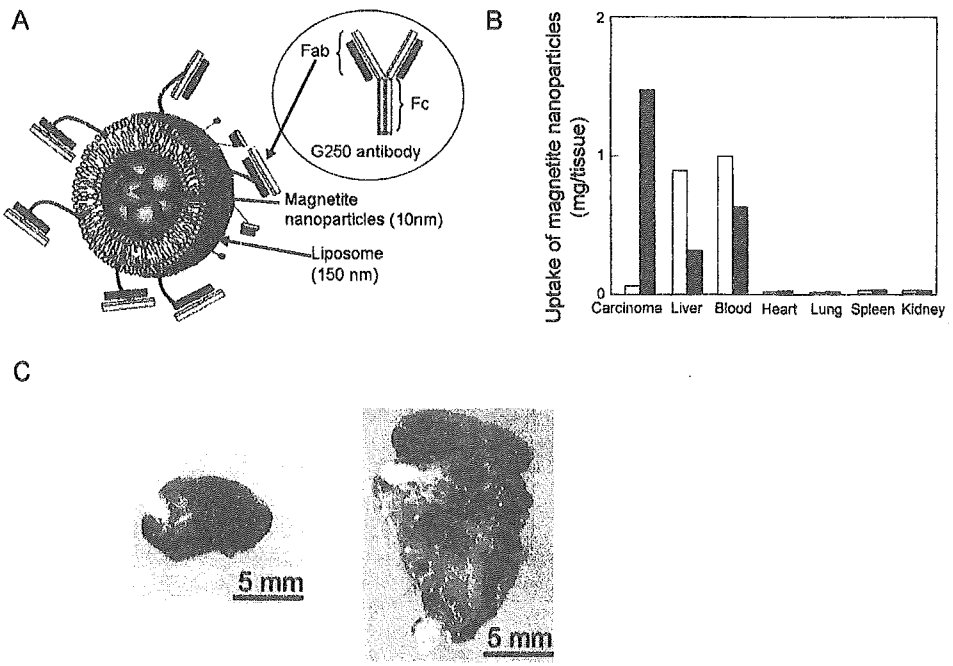

FIG. 4. Antibody-conjugated magnetoliposomes (AMLs) for active targeting. Magnetite nanoparticles were wrapped in a neutral liposome, and a G250 antibody was covalently linked to the liposomal surface (A). (B) Magnetite uptake of G250-AMLs for carcinomas and various organs 48 h after the intraarterial injection of AML (0.4 ml, net magnetite: 3 mg). Animals in group I (open columns), *i.e.*, the control group, were transplanted with MN antigen-overexpressing mouse renal cell carcinoma (MN-mRCC) and injected with magnetoliposomes (MLs). Group II animals (closed columns) were transplanted with MN-mRCC and the G250-AMLs were injected. (C) Photographs of a kidney 14 d after the hyperthermic treatment for MN-mRCC (left)- or mouse renal cell carcinoma without MN antigens (mRCC; right)-bearing mice. Forty-eight hours after the injection, the mice were exposed to a magnetic field (118 kHz and 384 Oe), and the treatment was repeated three times at 24-h intervals.

VI. ANTITUMOR IMMUNITY INDUCTION BY HYPERTHERMIA USING MAGNETITE NANOPARTICLES

Interestingly, Yanase *et al.* (48) observed that tumor-specific hyperthermia using magnetite nanoparticles induced antitumor immunity. They demonstrated this event by transplanting a tumor to each femur of a rat. MCLs were directly injected into only one tumor and the hyperthermic treatment was applied. The temperature at the MCL-injected tumor increased to 45°C, whereas that at the other tumor did not increase. However, both the tumors disappeared completely after 28 d (Fig. 5A). Immunocytochemical assay revealed that CD8-positive and CD4-positive T cells migrated to both tumors after the hyperthermic treatment. These results suggest that therapeutic magnetite nanoparticles are potentially effective tools for hyperthermic treatment of tumors, because in addition to the killing of tumor cells by heat, a host immune response is induced. To explain how tumor antigens are recognized by the host immune system, Kobayashi and coworkers (49–51) proposed heat shock protein (HSP)-mediated antitumor immunity as a mechanism.

Hyperthermia is known to induce HSPs (52). Since the expression of HSPs protects cells from heat-induced apoptosis (53), HSP expression is considered to be a complicating factor in hyperthermia. On the other hand, recent reports have shown the importance of HSPs, such as HSP70, HSP90 and glucose-regulated protein 96, in immune reactions. Furthermore, investigators have suggested that HSPs chaperone tumor antigens (54, 55). With regard to the mechanism of antitumor immunity induced by hyperthermia using MCLs, Kobayashi and coworkers (49, 50) have demonstrated two possible mechanisms of antigen presentation via HSP70 expression during hyperthermia. One possible mechanism is the presentation of antigenic peptides by the tumor cells via MHC class I molecules.

Srivastava and coworkers (56–58) proposed the following "relay line model" for tumor antigenic peptide transfer during antigen processing and presentation by HSPs: (i) The peptides are first bound to HSP70 (or HSP90), which are responsible for transporting them to the endoplasmic reticulum (ER) through the transporter associated with antigen processing (TAP); (ii) the peptides are transferred to gp96 in the lumen of the ER; (iii) in the terminal step, gp96 transfers the peptides to the MHC class I–β_2 microglobulin complexes. Wells and coworkers (59, 60) demonstrated that stably transfected B16 melanoma cells that constitutively expressed the human HSP70 exhibited significantly increased levels of the MHC class I antigens on their surface. Ito *et al.* (49) revealed that the augmentation of MHC class I antigens on the tumor cell surface via HSP70 expression caused the induction of immunity. The HSP70 expression level peaked 24 h after heating, and the augmentation of MHC class I surface expression level started 24 h after heating and peaked 48 h after heating. The expression of other immunologic mediators, such as intracellular adhesion molecule-1 (ICAM-1) and MHC class II antigens, did not increase. In an *in vivo* experiment using syngenic rats, the growth of the heated T-9 cells accompanied by the augmentation of MHC class I antigen surface expression level was significantly inhibited; on the other hand, the cells grew progressively in nude rats. Furthermore, in comparison with lymphocytes from non-immunized rats or rats injected with nonheated T-9 cells, the splenic lymphocytes of the rats injected with the heated T-9 cells displayed specific cytotoxicity against the T-9 cells. These results suggest that HSP70 is an important modulator

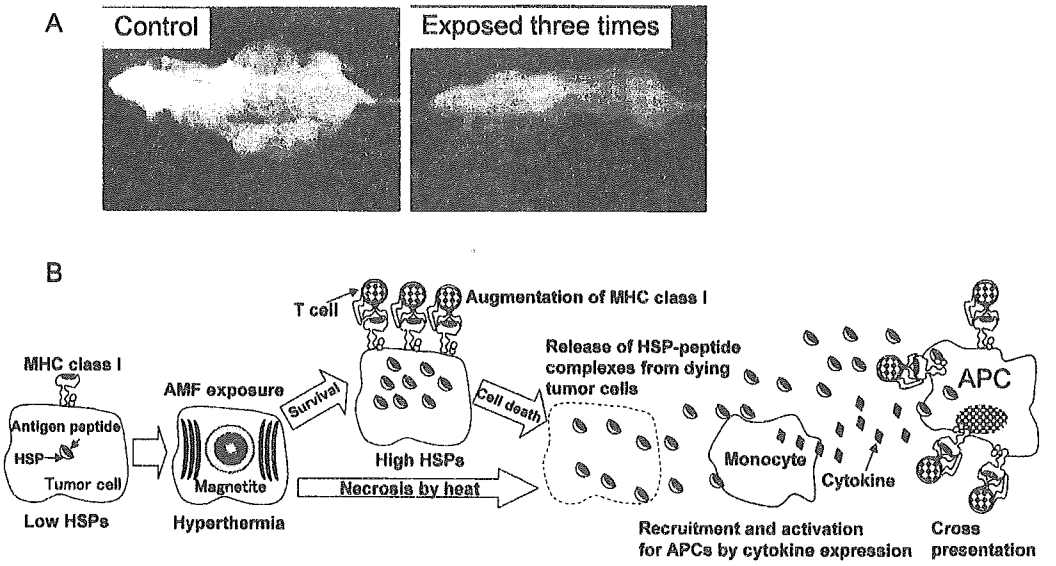

FIG. 5. Antitumor immune response induced by hyperthermia using magnetite nanoparticles. (A) Rats photographed on the 28th day after the MCL injection. Rat glioma T-9 cells (1×10^7 cells) were transplanted subcutaneously into the left femoral region of F344 rats. On the 9th day after transplantation into the left side, another aliquot of the T-9 cell suspension (1×10^7 cells) was transplanted subcutaneously into the right femoral region. The MCLs were injected into the left tumor only, on the 11th day after the first transplantation. When hyperthermic treatment was repeated three times at 24-h intervals, both tumors had disappeared by the 28th day after the MCL injection. (B) The hypothesis for the mechanism of immune response after hyperthermic treatment using magnetite nanoparticles. See text for details.

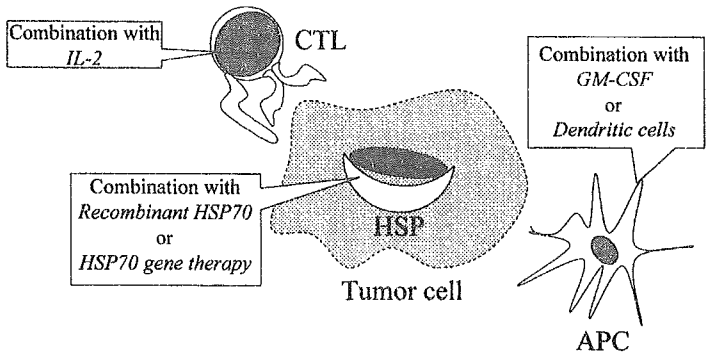

FIG. 6. Strategies for novel cancer immunotherapy based on the immune response induced by hyperthermia. Three key elements may be involved in this mechanism: (i) CD8-positive cytotoxic T lymphocytes (CTLs) as effector cells, (ii) APCs as antigen-processing and antigen-presenting cells for the HSP-peptide complexes released from necrotic cells, (iii) HSPs as natural and powerful immunostimulants. In order to enhance the antitumor immunity induced by hyperthermia, these three elements were combined with the hyperthermic treatment.

of tumor cell immunogenicity during hyperthermia.

An alternative mechanism for the recognition of tumor cell antigens by the host immune system in hyperthermia is the cross-presentation of antigenic peptides by professional antigen presenting cells (APCs). The HSP-mediated antitumor immunity may be caused by a vaccine-like effect of HSP–peptide complexes released from dying tumor cells. The released HSP–peptide complexes encounter APCs that express specific receptors such as CD91 (61). Interaction of HSP–peptide complexes with CD91 leads to receptor-mediated endocytosis, processing of the antigenic peptide by the endogenous MHC class I pathway, and the re-presentation of the peptide on the cell surface to the CD8-positive T cell receptor (61). Additionally, HSPs function as a direct activator of APCs, stimulating cytokine secretion from monocytes and inducing the maturation of dendritic cells (DCs) through CD14 and/or CD91 receptors (62). This cytokine-like ability of HSP70 to stimulate the innate immune system is independent of the peptides they chaperone, which suggests that HSP70 is a natural adjuvant. Ito *et al.* previously demonstrated that HSP70 expression following hyperthermia using MCLs induced antitumor immunity in T-9 rat glioma (50).

A proposed scenario in which HSPs function during the successive stages of an antitumor response after hyperthermia is summarized and illustrated in Fig. 5B. (i) Poorly immunogenic tumor cells, with a low concentration of intracellular HSP–peptide complexes, decreased the function of the endogenous antigen processing machinery and resulted in a very low level of MHC class I–peptide complexes at the cell surface. (ii) A sublethal stress response induced by hyperthermia using MCLs results in elevated levels of intracellular HSP–peptide complexes, enhanced processing of endogenous antigens, and an increase in the density of MHC class I–peptide complexes on the cell surface. These tumor cells are then recognized directly by MHC class I-restricted, tumor-specific T cells. (iii) Dying tumor cells, which are killed by the tumor-specific T-cells or by lethal hyperthermic treatment, release their intracellular contents, including HSP–peptide complexes. (iv) The released HSPs and/or antigenic peptides activate neighboring monocytes to produce proinflammatory cytokines and recruit APCs. (v) The HSP–peptide complexes are taken up by DCs and in turn presented to tumor-specific T-cells via MHC class I molecules (cross-presentation).

Recently, a vaccine consisting of the autologous tumor-derived heat shock protein gp96–peptide complexes (HSPPC-96, Oncophage; Antigenics, Woburn, MA, USA) has entered clinical trials, and the feasibility of treatment in metastatic melanoma patients was demonstrated (63). Since the HSP–peptide complexes have to be extracted from tumors in the body, surgery is required in this therapeutic protocol. The surgery and extraction will be unnecessary if the hyperthermia is induced by MCLs. Udono and Srivastava (64) reported that the vaccination effect of HSP–peptide complexes was directly dependent on the dose. When the HSPs in the tumor are regarded as an antigen source, 1 g (approximately 10^8 cells) of tumor tissue may contain approximately 2 mg of HSP70. This represents a much higher dose than that used for the clinical trials. In the hyperthermic system using MCLs, the expression of HSP70 was enhanced, and tissue lysis via necrosis was observed throughout the tumor. This hyperthermic system can produce HSP–peptide complexes (possibly including HSPs such as HSP90 and gp 96), resulting in vaccination therapy. From these results and some hypotheses mentioned above, it is expected that hyperthermia can be combined with cytokines to improve the effectiveness of cancer therapy. In fact, combinations with cytokines (IL-2 and GM-CSF) (65), heat-inducible TNF-α gene therapy (66), recombinant HSP70 (67), HSP70 gene therapy (68), and dendritic cell therapy (69), have been performed and significantly improved results were obtained, as shown in Fig. 6.

VII. TISSUE ENGINEERING USING MAGNETIC NANOPARTICLES

Tissue engineering holds great promise as a means of resolving various issues surrounding organ transplantation (70). Since cells labeled with magnetic nanoparticles can be manipulated using magnets, a novel tissue engineering methodology using magnetic force and functionalized magnetic nanoparticles referred to as Mag-TE was proposed by Ito *et al.* (71).

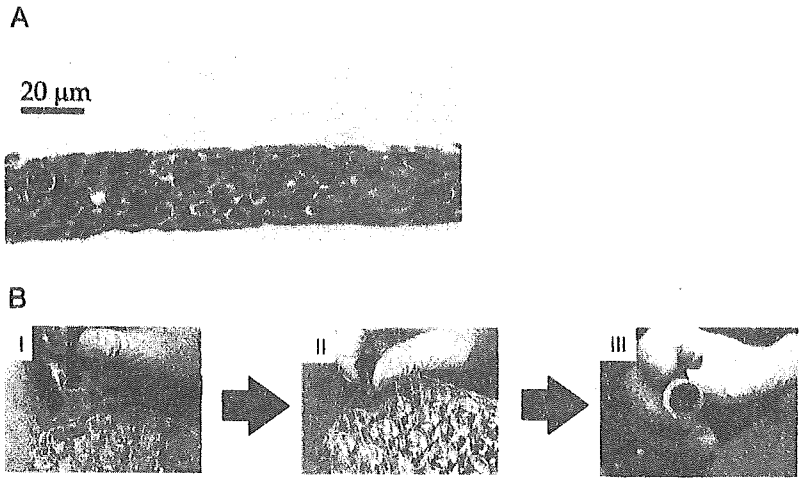

FIG. 7. Construction and harvesting of multilayered keratinocyte sheets using magnetite nanoparticles and a magnetic force. (A) Photographs of hematoxylin and eosin-stained cross sections of keratinocyte sheets constructed using MCLs and a magnet. Keratinocytes were incubated in an MCL-containing medium for 4 h (50 pg/cell) and then seeded onto ultra low-attachment plates with a magnet. The keratinocytes were cultured using a low-calcium medium (HuMedia-KG2; calcium concentration, 0.15 mM) for 24 h. (B) Recovery of keratinocyte sheets using magnets. In order to harvest the magnetically labeled keratinocyte sheets, the magnet positioned on the reverse side of the 24-well ultra low-attachment plate was removed, and a hydrophilically treated PVDF membrane was placed on top of the cylindrical alnico magnet (I). The magnet was positioned at the surface of the culture medium (II). Due to the magnetic force, the keratinocyte sheets floated up to the surface of the culture medium and stuck to the PVDF membrane (III).

It is possible to culture the principal cell (the keratinocyte) of the epidermis and to use these cells to reconstitute human tissue (72, 73). MCLs were used to magnetically label human keratinocytes, and Ito *et al.* (71) showed that magnetically labeled keratinocytes were accumulated using a magnet, and stratification was promoted by a magnetic force to form a sheet-like 3D construct. The addition of MCLs to human keratinocytes resulted in the rapid uptake of magnetite nanoparticles, and the amount of MCLs accumulated in the keratinocytes reached a maximum of 70% of the total added MCLs. Magnetically labeled keratinocytes were seeded into 24-well ultra low-attachment plates, the surface of which comprised a covalently bound hydrogel layer that is hydrophilic and neutrally charged. A neodymium magnet was placed under the plate. Keratinocytes without MCLs, or with MCLs in the absence of a magnet, did not attach onto the plates. In contrast, in the presence of the magnet, the keratinocytes with MCLs accumulated evenly throughout the wells (Fig. 7A). Ito *et al.* (71) investigated whether the magnetically labeled sheets could be harvested using magnets. Figure 7B shows the procedure for harvesting keratinocyte sheets constructed by Mag-TE. The magnet positioned at the reverse side of the plate was removed. Then, a hydrophilically treated PVDF membrane was placed on top of a cylindrical alnico magnet (Fig. 7B-I), and the magnet was positioned on the surface of the culture medium (Fig. 7B-II). Due to the magnetic force, the keratinocyte sheets floated up to the surface of the culture medium without disruption and stuck to the PVDF membrane, as shown in Fig. 7B-III.

Tissues and organs *in vivo* often comprise several types of cell layers. Cell–cell interactions among these cell layers are important in order to maintain the normal physiology of organ systems. Heterotypic interactions play a fundamental role in liver function (74, 75). Various 2D coculture systems of hepatocytes and nonparenchymal cells have been investigated (76, 77). However, novel technologies are required to reconstruct the liver to enable it to function similarly to *in vivo* conditions. Ito *et al.* (78) applied the Mag-TE technique, in which a magnetic force was used to precisely place magnetically labeled cells onto target cells and to promote heterotypic cell–cell adhesion to form a 3D construct. Human aortic endothelial cells (HAECs) were magnetically labeled using MCLs, and the labeled HAECs were positioned onto a rat hepatocyte layer using a magnetic force. When a magnet was placed under the culture plate, HAECs accumulated on the hepatocyte layer. They found a construct consisting of a hepatocyte monolayer that expressed albumin under thick HAEC layers (Fig. 8A). To determine the cellular function in the layered coculture system using the magnet, the hepatic albumin expression was measured (Fig. 8B). Albumin secretion in the homotypic hepatocyte culture was undetectable beyond 5 d of culture. On the other hand, in the presence of a magnetic force, layered cocultures maintained a high level of albumin secretion throughout the study.

In conclusion, Ito *et al.* (71) developed a novel methodology to construct 3D tissues similar to those of *in vivo* tissues using magnetic nanoparticles and a magnetic force referred to as Mag-TE. This technology is presently being applied to various cell types such as human mesenchymal stem cells (79) and retinal pigment epithelial cells (80). These results suggest that Mag-TE is a promising approach for tissue engineering.

VIII. CONCLUSION

In this article, we discuss the application of magnetic nanoparticles in magnetic separation, cancer diagnosis (MRI), hyperthermia and tissue engineering. These tech-

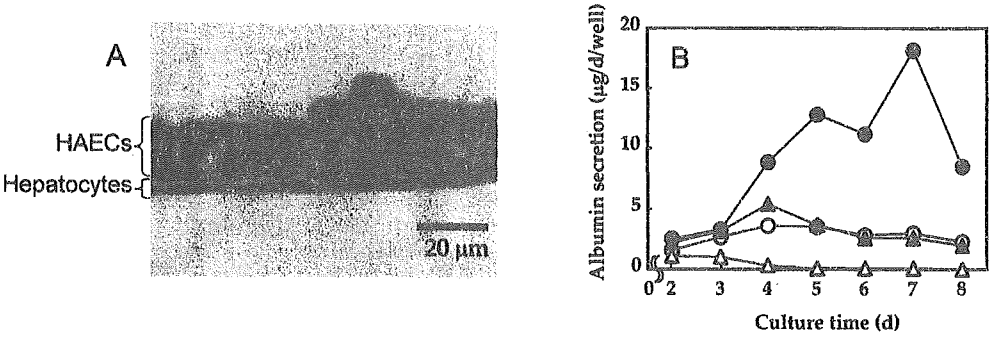

FIG. 8. Construction of 3D coculture of HAECs and hepatocytes using magnets. HAECs were incubated for 8 h in a medium containing MCLs and seeded onto rat hepatocyte monolayers, after which the magnet was positioned. (A) Photographs of cells immunohistochemical stained for albumin double-stained with Berlin blue. (B) Albumin secretion by rat hepatocytes under different culture conditions. Hepatocytes were initially cultured for 2 d to allow the formation of monolayers. Open triangles, Hepatocytes incubated alone as homotypic cultures; closed triangles, HAECs seeded onto hepatocytes; open circles, HAECs labeled with MCLs seeded onto hepatocytes without magnets; closed circles, HAECs labeled with MCLs seeded onto hepatocytes with magnets and then cultured for 8 d.

niques are addressed in an interdisciplinary manner based on biochemistry, electronics and magnetics, and physiology. Currently, magnetic techniques are complementary to other methods used in medical applications and the combination of these methods should result in a more effective therapeutic approach.

ACKNOWLEDGMENTS

This study was partially funded by Grants-in-Aid for Scientific Research (no. 13853005) from the Ministry of Education, Culture, Sports, Science and Technology of Japan.

REFFERENCES

1. **Dunnill, P. and Lilly, M. D.:** Purification of enzymes using magnetic bioaffinity materials. Biotechnol. Bioeng., **16**, 987–990 (1974).
2. **Mosbach, K. and Anderson, L.:** Magnetic ferrofluids for prepareation of magnetic polymers and their application in affinity chromatography. Nature, **270**, 259–261 (1977).
3. **Stechell, C. H.:** Magnetic separations in biotechnology — a review. J. Chem. Technol. Biotechnol., **35B**, 175–182 (1985).
4. **Kondo, A., Kamura, H., and Higashitani, K.:** Development and application of thermosensitive magnetic immunomicrospheres for antibody purification. Appl. Microbiol. Biotechnol., **41**, 99–105 (1994).
5. **Kondo, A. and Fukuda, H.:** Preparation of thermo-sensitive magnetic hydrogel microspheres and application to enzyme immobilization. J. Ferment. Bioeng., **84**, 337–341 (1997).
6. **Häfeli, U., Shutt, W., Teller, J., and Zborowski, M. (ed.):** Scientific and clinical application of magnetic carriers. Plenum Press, New York (1997).
7. **Safarik, I. and Safarikova, M.:** Use of magnetic techniques for isolation of cells. J. Chromatogr. B Biomed. Sci. Appl., **722**, 33–53 (1999).
8. **Saiyed, Z. M., Telang, S. D., and Racnchand, C. N.:** Application of magnetic techniques in the field of drug discovery and biomedicine. Biomagn. Res. Technol., **1**, 23–33 (2003).
9. **Safarik, I. and Safarikova, M.:** Magnetic techniques for the isolation and purification of proteins and peptides. Biomagn. Res. Technol., **2**, 7–34 (2004).
10. **Liu, C.-Z., Honda, H., Ohshima, A., Shinkai, M., and Kobayashi, T.:** Development of chitosan-magnetite aggregates containing *Nitrosomonas europaea* cells for nitrification enhancement. J. Biosci. Bioeng., **89**, 420–425 (2000).
11. **Barclay, A. N., Brown, M. L., Beyers, A. D., Davis, S. J., Somoza, C., and Williams, A. F.:** The leukocytes antigen facts book. Academic Press, San Diego, CA (1993).
12. **Weber, C. and Falkenhagen, D.:** Specific blood purification by means of antibody-conjugated magnetic microspheres, p. 371–378. *In* Häfeli, U., Shutt, W., Teller, J., and Zborowski, M. (ed.), Scientific and clinical application of magnetic carriers. Plenum Press, New York (1997).
13. **Guesdon, J. L., Thiery, R., and Avrameas, S.:** Magnetic enzyme immunoassay for measuring human IgE. J. Allergy Clin. Immnol., **6**, 23–27 (1978).
14. **Druet, E., Mahieu, P., Foidart, J. M., and Druet, P.:** Magnetic solid-phase enzyme immunoassay for the detection of anti-glomerular basement membrane antibodies. J. Immnol. Methods, **48**, 149–157 (1982).
15. **Pazzagli, M., Kohen, F., Sufi, S., Masironi, B., and Cekan, S. Z.:** Immunometric assay for lutropin (hLH) based on the use of universal reagents for enzymatic labeling and magnetic separation and monitored by enhanced chemiluminescence. J. Immunol. Methods, **114**, 62–68 (1988).
16. **Vonk, G. P. and Schram, J. L.:** Dual-enzyme cascade-magnetic separation immunoassay for respiratory syncytial virus. J. Immunol. Methods, **137**, 133–139 (1991).
17. **Shinkai, M., Wang, J., Kamihira, M., Iwata, M., Honda, H., and Kobayashi, T.:** Rapid enzyme-linked immunosorbent assay with functional magnetite particles. J. Ferment. Bioeng., **73**, 166–168 (1992).
18. **Nagatani, N., Shinkai, M., Honda, H., and Kobayashi, T.:** Development of a new transformation method using magnetite cationic liposomes and magnetic selection of transformed cells. Biotechnol. Lett., **22**, 999–1002 (2000).
19. **Padmanabhan, R., Corsico, C. D., Howard, T. H., Holter, W., Fordis, C. M., Willingham, M., and Howard, B. H.:** Purification of transiently transfected cells by magnetic affinity cell sorting. Anal. Biochem., **170**, 341–348 (1988).
20. **Schneider, S. and Rusconi, S.:** Magnetic selection of transiently transfected cells. Biotechniques, **21**, 876–880 (1996).
21. **Bergemann, C., Müller-Schulte, D., Oster, J., à Brassard, L., and Lübbe, A. S.:** Magnetic ion-exchange nano- and microparticles for medical, biochemical and molecular biological applications. J. Magn. Magn. Matel., **194**, 45–52 (1999).
22. **Magin, R. L., Wright, S. M., Niesman, M. R., Chan, H. C., and Swartz, H. M.:** Liposome delivery of NMR contrast agents for improved tissue imaging. Magn. Reson. Med., **3**, 440–447 (1986).
23. **Gillis, P. and Koenig, S. H.:** Transverse relaxation of solvent protons induced by magnetized spheres: application to ferritin, erythrocytes, and magnetite. Magn. Reson. Med., **5**,

323–345 (1987).
24. **Saini, S., Stark, D. D., Hahn, P. F., Wittenberg, J., Brady, T. J., and Ferrucci, J. T.:** Ferrite particles: a superparamagnetic MR contrast agent for the reticuloendothelial system. Radiology, **162**, 211–216 (1987).
25. **Stark, D. D., Weissleder, R., Elizondo, G., Hahn, P. F., Saini, S., Todd, L. E., Wittenberg, J., and Ferrucci, J. T.:** Superparamagnetic iron oxide: clinical application as a contrast agent for MR imaging of the liver. Radiology, **168**, 297–301 (1988).
26. **Suzuki, M., Honda, H., Kobayashi, T., Wakabayashi, T., Yoshida, J., and Takahashi, M.:** Development of a target-directed magnetic resonance contrast agent using monoclonal antibody-conjugated magnetic particles. Brain Tumor Pathol., **13**, 127–132 (1996).
27. **Shinkai, M., Ohshima, A., Yanase, M., Uchiyama, T., Mohri, K., Wakabayashi, T., Yoshida, J., Honda, H., and Kobayashi, T.:** Development of novel magnetic sensing for brain lesion using functional magnetic particles. Kagaku Kougaku Ronbunshu, **24**, 174–178 (1998).
28. **Uchiyama, T., Mohri, K., Shinkai, M., Ohshima, A., Honda, H., Kobayashi, T., Wakabayashi, T., and Yoshida, J.:** Basic study for brain tumor position sensing using amorphous wire MI micro magnetic sensor. Trans. IEE, Jpn., **119-C**, 545–553 (1999).
29. **Cavaliere, R., Ciocatto, E. C., Giovanella, B. C., Heidelburger, C., Jonson, R. O., Margottini, M., Mondovi, B., Moricca, B. G., and Rossi-Fanelli, A.:** Selective heat sensitivity of cancer cells. Biochemical and clinical studies. Cancer, **20**, 1351–1381 (1967).
30. **Stauffer, P. R., Cetas, T. C., Fletcher, A. M., DeYoung, D. W., Dewhirst, M. W., Oleson, J. R., and Roemer, R. B.:** Observations on the use of ferromagnetic implants for inducing hyperthermia. IEEE Trans. Biomed. Eng., **31**, 76–90 (1984).
31. **Lin, J. C. and Wang, Y. J.:** Interstitial microwave antennas for thermal therapy. Int. J. Hyperthermia, **3**, 37–47 (1987).
32. **Ikeda, N., Hayashida, O., Kameda, H., Ito, H., and Matsuda, T.:** Experimental study on thermal damage to dog normal brain. Int. J. Hyperthermia, **10**, 553–561 (1994).
33. **Jordan, A., Wust, P., Fähling, H., John, W., Hinz, A., and Felix, R.:** Inductive heating of ferrimagnetic particles and magnetic fluids: physical evaluation of their potential for hyperthermia. Int. J. Hyperthermia, **9**, 51–68 (1993).
34. **Mitsumori, M., Hiraoka, M., Shibata, T., Okuno, Y., Nagata, Y., Nishimura, Y., Abe, M., Hasegawa, M., Nagae, H., and Ebisawa, Y.:** Development of intra-arterial hyperthermia using a dextran-magnetite complex. Hepatogastroenterology, **43**, 1431–1437 (1996).
35. **Wada, S., Yue, L., Tazawa, K., Furuta, I., Nagae, H., Takemori, S., and Minamimura, T.:** New local hyperthermia using dextran magnetite complex (DM) for oral cavity: experimental study in normal hamster tongue. Oral Dis., **7**, 192–195 (2001).
36. **Gordon, R. T., Hines, J. R., and Gordon, D.:** Intracellular hyperthermia. A biophysical approach to cancer treatment via intracellular temperature and biophysical alterations. Med. Hypothesis, **5**, 83–102 (1979).
37. **Jordan, A., Wust, P., Scholz, R., Tesch, B., Fähling, H., Mitrovics, T., Vogl, T., Cervós-Navarro, J., and Felix, R.:** Cellular uptake of magnetic fluid particles and their effects on human adenocarcinoma cells exposed to AC magnetic fields *in vitro*. Int. J. Hyperthermia, **12**, 705–722 (1996).
38. **Chan, D. C. F., Kirpotin, D. B., and Bunn, P. A.:** Synthesis and evaluation of colloidal magnetic iron-oxides for the site-specific radiofrequency-induced hyperthermia of cancer. J. Magn. Magn. Mater., **122**, 374–378 (1993).
39. **Shinkai, M., Matsui, M., and Kobayashi, T.:** Heat properties of magnetoliposomes for local hyperthermia. Jpn. J. Hyperthermic Oncol., **10**, 168 (1994).
40. **Shinkai, M., Yanase, M., Honda, H., Wakabayashi, T., Yoshida, J., and Kobayashi, T.:** Intracellular hyperthermia for cancer using magnetite cationic liposome: *in vitro* study. Jpn. J. Cancer Res., **87**, 1179–1183 (1996).
41. **Suzuki, M., Shinkai, M., Honda, H., and Kobayashi, T.:** Anticancer effect and immune induction by hyperthermia of malignant melanoma using magnetite cationic liposomes. Melanoma Res., **13**, 129–135 (2003).
42. **Yanase, M., Shinkai, M., Honda, H., Wakabayashi, T., Yoshida, J., and Kobayashi, T.:** Intracellular hyperthermia for cancer using magnetite cationic liposomes: an *in vivo* study. Jpn. J. Cancer Res., **89**, 463–469 (1998).
43. **Matsuoka, F., Shinkai, M., Honda, H., Kubo, T., Sugita, T., and Kobayashi, T.:** Hyperthermia using magnetite cationic liposomes for hamster osteosarcoma. Biomagn. Res. Technol., **2**, 3 (2004).
44. **Matsuno, H., Tohnai, I., Mitsudo, K., Hayashi, Y., Ito, M., Shinkai, M., Kobayashi, T., Yoshida, J., and Ueda, M.:** Interstitial hyperthermia using magnetite cationic liposomes inhibit to tumor growth of VX-7 transplanted tumor in rabbit tongue. Jpn. J. Hyperthermic Oncol., **17**, 141–149 (2001).
45. **Ito, A., Tanaka, K., Honda, H., Abe, S., Yamaguchi, H., and Kobayashi, T.:** Complete regression of mouse mammary carcinoma with a size greater than 15 mm by frequent repeated hyperthermia using magnetite nanoparticles. J. Biosci. Bioeng., **96**, 364–369 (2003).
46. **Le, B., Shinkai, M., Kitade, T., Honda, H., Yoshida, J., Wakabayashi, T., and Kobayashi, T.:** Preparation of tumor-specific magnetoliposomes and their application for hyperthermia. J. Chem. Eng. Jpn., **34**, 66–72 (2001).
47. **Shinkai, M., Le, B., Honda, H., Yoshikawa, K., Shimizu, K., Saga, S., Wakabayashi, T., Yoshida, J., and Kobayashi, T.:** Targeting hyperthermia for renal cell carcinoma using human MN antigen-specific magnetoliposomes. Jpn. J. Cancer Res., **92**, 1138–1145 (2001).
48. **Yanase, M., Shinkai, M., Honda, H., Wakabayashi, T., Yoshida, J., and Kobayashi, T.:** Antitumor immunity induction by intracellular hyperthermia using magnetite cationic liposomes. Jpn. J. Cancer Res., **89**, 775–782 (1998).
49. **Ito, A., Shinkai, M., Honda, H., Wakabayashi, T., Yoshida, J., and Kobayashi, T.:** Augmentation of MHC class I antigen presentation via heat shock protein expression by hyperthermia. Cancer Immmunol. Immunother., **50**, 515–522 (2001).
50. **Ito, A., Shinkai, M., Honda, H., Yoshikawa, K., Saga, S., Wakabayashi, T., Yoshida, J., and Kobayashi, T.:** Heat shock protein 70 expression induces antitumor immunity during intracellular hyperthermia using magnetite nanoparticles. Cancer Immunol. Immunother., **52**, 80–88 (2003).
51. **Ito, A., Honda, H., and Kobayashi, T.:** Cancer immunotherapy based on intracellular hyperthermia using magnetite nanoparticles: a novel concept of "heat-controlled necrosis" with heat shock protein expression. Cancer Immunol. Immunother. (2005). (in press)
52. **Schlesinger, M. J.:** Heat shock proteins. J. Biol. Chem., **265**, 12111–12114 (1990).
53. **Mosser, D. D., Caron, A. W., Bourget, L., Meriin, A. B., Sherman, M. Y., Morimoto, R. I., and Massie, B.:** The chaperone function of hsp70 is required for protection against stress-induced apoptosis. Mol. Cell. Biol., **20**, 7146–7159 (2000).
54. **Ménoret, A. and Chandawarkar, R.:** Heat-shock protein-based anticancer immunotherapy: an idea whose time has come. Semin. Immunol., **25**, 654–660 (1998).
55. **Srivastava, P. K., Ménoret, A., Basu, S., Binder, R., and Quade, K.:** Heat shock proteins come of age: primitive functions acquire new roles in an adaptive world. Immunity, **8**, 657–665 (1998).
56. **Srivastava, P. K. and Maki, R. G.:** Stress-induced proteins in

immune response to cancer. Curr. Top. Microbiol. Immunol., **167**, 109–123 (1991).
57. **Srivastava, P. K. and Heike, M.:** Tumor-specific immunogenicity of stress-induced proteins: convergence of two evolutionary pathways of antigen presentation? Semin. Immunol., **3**, 57–64 (1993).
58. **Srivastava, P. K., Udono, H., Blachere, N. E., and Li, Z.:** Heat shock proteins transfer peptides during antigen processing and CTL priming. Immunogenetics, **39**, 93–98 (1994).
59. **Wells, A. D. and Malkovsky, M.:** Heat shock proteins, tumor immunogenicity and antigen presentation: an integrated view. Immunol. Today, **21**, 129–132 (2000).
60. **Wells, A. D., Rai, S. K., Salvato, M. S., Band, H., and Malkovsky, M.:** Hsp72-mediated augmentation of MHC class I surface expression and endogenous antigen presentation. Int. Immunol., **10**, 609–617 (1998).
61. **Basu, S., Binder, R. J., Ramalingam, T., and Srivastava, P. K.:** CD91 is a common receptor for heat shock proteins gp96, hsp90, hsp70, and calreticulin. Immunity, **14**, 303–313 (2001).
62. **Asea, A., Kraeft, S. K., Kurt-Jones, E. A., Stevenson, M. A., Chen, L. B., Finberg, R. W., Koo, G. C., and Calderwood, S. K.:** HSP70 stimulates cytokine production through a CD14-dependant pathway, demonstrating its dual role as a chaperone and cytokine. Nat. Med., **6**, 435–442 (2000).
63. **Belli, F., Testori, A., Rivoltini, L., Maio, M., Andreola, G., Sertoli, M. R., Gallino, G., Piris, A., Cattelan, A., Lazzari, I., and other 19 authors:** Vaccination of metastatic melanoma patients with autologous tumor-derived heat shock protein gp96-peptide complexes: clinical and immunologic findings. J. Clin. Oncol., **20**, 4169–4180 (2002).
64. **Udono, H. and Srivastava, P. K.:** Heat shock protein 70-associated peptides elicit specific cancer immunity. J. Exp. Med., **178**, 1391–1396 (1993).
65. **Ito, A., Tanaka, K., Kondo, K., Shinkai, M., Honda, H., Matsumoto, K., Saida, T., and Kobayashi, T.:** Tumor regression by combined immunotherapy and hyperthermia using magnetic nanoparticles in an experimental subcutaneous murine melanoma. Cancer Sci., **94**, 308–313 (2003).
66. **Ito, A., Shinkai, M., Honda, H., and Kobayashi, T.:** Heat-inducible TNF-alpha gene therapy combined with hyperthermia using magnetic nanoparticles as a novel tumor-targeted therapy. Cancer Gene Ther., **8**, 649–654 (2001).
67. **Ito, A., Matsuoka, F., Honda, H., and Kobayashi, T.:** Antitumor effects of combined therapy of recombinant heat shock protein 70 and hyperthermia using magnetic nanoparticles in an experimental subcutaneous murine melanoma. Cancer Immunol. Immunother., **53**, 26–32 (2004).
68. **Ito, A., Matsuoka, F., Honda, H., and Kobayashi, T.:** Heat shock protein 70 gene therapy combined with hyperthermia using magnetic nanoparticles. Cancer Gene Ther., **10**, 918–925 (2003).
69. **Tanaka, K., Ito, A., Kobayashi, T., Kawamura, T., Shimada, S., Matsumoto, K., Saida, T., and Honda, H.:** Intratumoral injection of immature dendritic cells enhances antitumor effect of hyperthermia using magnetic nanoparticles. Int. J. Cancer, **116**, 624–633 (2005).
70. **Langer, R. and Vacanti, J. P.:** Tissue engineering. Science, **260**, 920–926 (1993).
71. **Ito, A., Hayashida, M., Honda, H., Hata, K., Kagami, H., Ueda, M., and Kobayashi, T.:** Construction and harvest of multilayered keratinocyte sheets using magnetite nanoparticles and magnetic force. Tissue Eng., **10**, 873–880 (2004).
72. **Yannas, I. V., Burke, J. F., Orgill, D. P., and Skrabut, E. M.:** Wound tissue can utilize a polymeric template to synthesize a functional extension of skin. Science, **215**, 174–176 (1982).
73. **Bell, E., Ehrlich, H. P., Buttle, D. J., and Nakatsuji, T.:** Living tissue formed in vitro and accepted as skin-equivalent tissue of full thickness. Science, **211**, 1052–1054 (1981).
74. **Houssaint, E.:** Differentiation of the mouse hepatic primordium. I. An analysis of tissue interactions in hepatocyte differentiation. Cell Differ., **9**, 269–279 (1980).
75. **Douarin, N. M.:** An experimental analysis of liver development. Med. Biol., **53**, 427–455 (1975).
76. **Bhatia, S. N., Yarmush, M. L., and Toner, M.:** Controlling cell interactions by micropatterning in cocultures: hepatocytes and 3T3 fibroblasts. J. Biomed. Mater. Res., **34**, 189–199 (1997).
77. **Yamato, M., Kwon, O. H., Hirose, M., Kikuchi, A., and Okano, T.:** Novel patterned cell coculture utilizing thermally responsive grafted polymer surfaces. J. Biomed. Mater. Res., **55**, 137–140 (2001).
78. **Ito, A., Takizawa, Y., Honda, H., Hata, K., Kagami, H., Ueda, M., and Kobayashi, T.:** Tissue engineering using magnetite nanoparticles and magnetic force: heterotypic layers of cocultured hepatocytes and endothelial cells. Tissue Eng., **10**, 833–840 (2004).
79. **Ito, A., Hibino, E., Honda, H., Hata, K., Kagami, H., Ueda, M., and Kobayashi, T.:** A new methodology of mesenchymal stem cell expansion using magnetic nanoparticles. Biochem. Eng. J., **20**, 119–125 (2004).
80. **Ito, A., Hibino, E., Kobayashi, C., Terasaki, H., Kagami, H., Ueda, M., Kobayashi, T., and Honda, H.:** Construction and delivery of tissue-engineering human retinal pigment epithelial cell sheets using magnetite nanoparticles and manetic force. Tissue Eng., **11**, 489–496 (2005).

The Prostate 64:373–381 (2005)

Anticancer Effect of Hyperthermia on Prostate Cancer Mediated by Magnetite Cationic Liposomes and Immune-Response Induction in Transplanted Syngeneic Rats

Noriyasu Kawai,[1]* Akira Ito,[2] Yoko Nakahara,[2] Mitsuru Futakuchi,[3] Tomoyuki Shirai,[3] Hiroyuki Honda,[2] Takeshi Kobayashi,[2] and Kenjiro Kohri[1]

[1]Department of Nephro-urology, Nagoya City University Graduate School of Medical Sciences, Nagoya, Japan
[2]Department of Biotechnology, School of Engineering, Nagoya University, Nagoya, Japan
[3]Department of Experimental Oncology and Tumor Biology, Nagoya City University Graduate School of Medical Sciences, Nagoya, Japan

BACKGROUND. The hyperthermic effect of magnetic particles was examined in rat prostate cancer in vivo. Magnetic cationic liposomes (MCLs) have a positive surface charge and generate heat in an alternating magnetic field (AMF) due to hysteresis losses.

METHODS. Rat prostate cancer cells (PLS 10; androgen independent) were injected subcutaneously into the flank of F344 rats. MCLs were injected into rat prostate cancer nodules that had grown to 5–6 mm in diameter, and were then exposed to an AMF. Tumor growth rates were measured. To examine whether hyperthermia caused immune induction for PLS 10, cytotoxicity assays and immunohistochemical staining for CD3, CD4, CD8, and Heat Shock Protein (HSP) 70 were performed.

RESULT. The tumor temperature increased to 45°C whereas the body temperature remained at around 38°C. Tumor regression was observed in the hyperthermic group. CD3, CD4, and CD8 immunocytes were present in the tumor tissues of the rats exposed to hyperthermia, but they were not detected in any of the tumor tissue of untreated rats. HSP70 also appeared in the viable area at its boundary with the necrotic area. The cytotoxic activity of tumor-transplanted rats for PLS 10 cells increased in hyperthermic-treatment rats.

CONCLUSION. These results suggest that hyperthermia using MCLs is an effective therapy for prostate cancer, since this treatment appears to kill the prostate cancer cells not only directly by heating but also by inducing an immune response. This therapy may cure not only the primary lesion but also metastatic lesions. *Prostate 64: 373–381, 2005.* © 2005 Wiley-Liss, Inc.

KEY WORDS: **prostate cancer; hyperthermia; magnetite cationic liposome; immune-response induction**

INTRODUCTION

Prostate cancer is the most frequently diagnosed malignancy in Western males and its incidence is increasing rapidly in Japan [1]. This increase is believed to be attributable to longer life expectancy, growing prostate awareness, and more intense screening [2,3].

The success of early prostate cancer detection has resulted in an increased number of candidates for therapy. The main treatment options for clinically localized prostate cancer currently consist of surgical extirpation and radiation therapy (external beam radiation therapy and/or brachytherapy) [4]. There are instances in which radical prostatectomy is not an

*Correspondence to: Noriyasu Kawai, Department of Nephro-urology, Nagoya City University Graduate School of Medical Sciences, 1 Kawasumi, Mizuho-cho, Mizuho-ku, Nagoya 467-8601, Japan. E-mail: norikawa@med.nagoya-cu.ac.jp
Received 30 October 2004; Accepted 21 December 2004
DOI 10.1002/pros.20253
Published online 7 March 2005 in Wiley InterScience (www.interscience.wiley.com).

option, such as when the patient is a poor risk for surgery or due to the wishes of the patient, in which cases radiation treatment becomes an option. Hormonal therapy, careful observation, or combination therapy with these methods are also options. Decisions regarding treatment must be made on an individual basis, with consideration for the patient's life expectancy and quality of life, as well as the patient's wishes [5].

Some other treatment options are less popular: cryotherapy [6–8], high-intensity focused ultrasound [9–11], and hyperthermia. The preliminary data suggest that high-intensity focused ultrasound represents a valid alternative treatment strategy for patients with localized prostate cancer who are unsuitable for surgery [9–11].

Cryosurgical ablation of the prostate is one approach to the treatment of localized prostate cancer. Third-generation cryosurgery uses gas-driven probes that enable the use of probe diameters of only 17 gauge, and this minimally invasive technique appears to be well tolerated. Cryosurgery has reemerged as an evolving technology and a minimally invasive treatment option. In 1996 the American Urological Association recognized cryoablation as a therapeutic option for prostate cancer in its position statement and removed the "investigational" label from this procedure.

Adding hyperthermia to conventional radiotherapy may also improve local control in prostate carcinoma. Hyperthermia is known to enhance the effect of radiation on prostate cancer cells in vitro [12]. Various hyperthermia techniques can be used to treat prostate carcinoma. Transurethral and/or transrectal hyperthermia produce a relatively uncontrollable heat distribution because of the limited heat penetration depth [13], and Algan et al. [14] reported no improvement in treatment outcome when using transrectal hyperthermia. The feasibility of interstitial [15] and regional hyperthermia for locally advanced prostate carcinoma has been reported [16–18], but these techniques require further development before they can be applied clinically.

Hyperthermia is based on the fact that tumor cells are more sensitive to heat than is healthy tissue [19]. However, it is difficult to specifically heat tumors with hyperthermia because the heating effects are influenced by various factors such as tumor size and the position of electrodes. In addition, the inevitable technical problem with hyperthermia is the difficulty of uniformly heating only the tumor region until the required temperature has been reached whilst not damaging normal tissue. Some researchers have investigated the application of submicron-sized magnetic particles for intracellular hyperthermia in order to overcome these disadvantages [20,21]. These magnetic particles generate heat under an alternating magnetic field (AMF) due to hysteresis losses [22]. We have developed "magnetite cationic liposomes" (MCLs) for inducing intracellular hyperthermia [23,24]. MCLs have been developed to improve adsorption and accumulation in the tumor cells, and have shown a tenfold higher affinity for the tumor cells than neutrally charged magnetoliposomes [24] due to electrostatic interaction with the negatively charged cell membrane. The hyperthermic effect of MCLs against some malignant tumor cells has been demonstrated in vivo [25]. Our hyperthermia procedure kills tumor cells not only directly by heating but also by the induction of an immune response [26].

In the study described in the present paper, we examined the hyperthermic effect of MCLs on rat prostate cancer in vivo, and demonstrated that our hyperthermic protocol can induce an antitumor immune response against rat prostate cancer.

MATERIALS AND METHODS

Tumor Cell Type and Animal Model

Cells were obtained from the rat prostate cancer cell line PLS 10, which has been established at Department of Experimental Oncology and Tumor Biology, Nagoya City University Graduate School of Medical Sciences [27] (Fig. 1A). This cell line has been established from 3,2'-dimethyl-4-aminobiphenyl plus testosterone-induced carcinomas in the dorsal prostate of male F344 rats. This cell line forms well-differentiated adenocarcinomas with abundant connective tissue stroma. PLS 10 cells are immunohistochemically negative for androgen receptors, and the growth of PLS 10 cells is androgen independent.

Four-week-old male F344 rats were purchased from Charles River Japan (Yokohama, Japan). To prepare tumor-bearing animals, cell suspensions including approximately 1×10^6 PLS 10 in 100 μl of phosphate buffer (0.05M sodium phosphate and 0.15M NaCl, pH 7.4) were injected subcutaneously into the right flank of F344 rat under short-term anesthesia by intraperitoneal injection of sodium pentobarbital (50 mg/kg body weight). Prostate cancer nodules that had grown to a diameter of about 5–6 mm were used for the experiments. The tumor diameter was measured every 3 days. The tumor volume was determined as Tumor volume $= 0.5 \times (\text{length} \times \text{width}^2)$.

The experimental protocol in the present study was approved by the Animal Care Committee of Nagoya City University Medical School. Animal experiments were performed according to the principles laid down in the "Guide for the Care and Use of Laboratory Animals" prepared under the direction of the Office of the Prime Minister of Japan. In this experiment, prostate cancer derived from the prostate of F344 rats

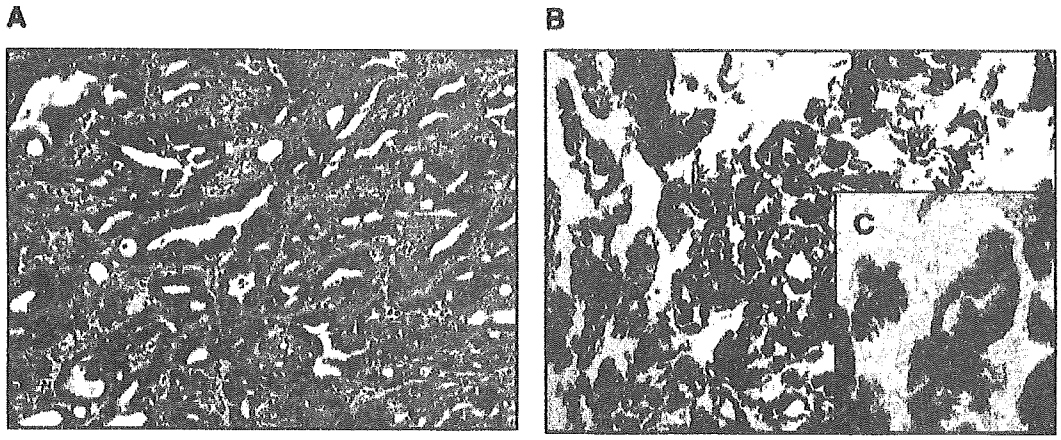

Fig. 1. **A**: Histology of rat prostate cancer cell line PLS 10. The tumor is a well-differentiated adenocarcinoma. H-E stain, ×200. **B**: Histology of a PLS 10 tumor injected with magnetic cationic liposomes (MCLs). Prostate glandular cells were stained by ferrous stain because MCLs were present in the prostate glandular cell but not on stromal tissue. Ferrous stain, ×200. **C**: Same as B, except ×400. [Color figure can be viewed in the online issue, which is available at www.interscience.wiley.com.]

are transplanted into syngeneic rats, which differs considerably from the experiment in which human tumor tissue is transplanted into nude mice. This experiment therefore represents an excellent model for evaluating host immune responses to tumor tissue.

Preparation of MCLs

The magnetic particles were kindly donated by Toda Kogyo (Hiroshima, Japan), and had an average diameter of 10 nm. MCLs were prepared by sonication as described previously with some modifications [23]. One milliliter of the colloidal magnetite (net 20 mg of magnetite) was coated with a lipid membrane comprising *N*-(α-trimethylammonioacetyl) didodecyl-D-glutamate chloride (Sogo Pharmaceutical, Tokyo) and dilauroylphosphatidylcholine and dioleoylphosphatidylethanolamine (Sigma Chemical, St. Louis, MO) at a molar ratio of 1:2:2, respectively. The magnetite concentration was measured by the potassium thiocyanate method [28].

Injection of MCLs and Heat Generation in an AMF

After the prostate cancer nodules had grown to 5–6 mm in diameter, a 26-G syringe needle containing MCLs was inserted longitudinally into each prostate cancer nodule subcutaneously from the nodule edge (Fig. 2A). Two grams of MCLs was injected using an infusion pump (SP100i; World Precision Instruments, Sarasota, FL) for 30 min (Fig. 1B). The rats were then separated into two groups: Group I mice were not exposed to an AMF (control group), whereas after injection of the MCLs, Group II rats were subjected once to hyperthermia for 30 min at 45°C. The AMF was created using a horizontal coil (inner diameter: 7 cm; length: 7 cm) with a transistor inverter (LTG-100-05;

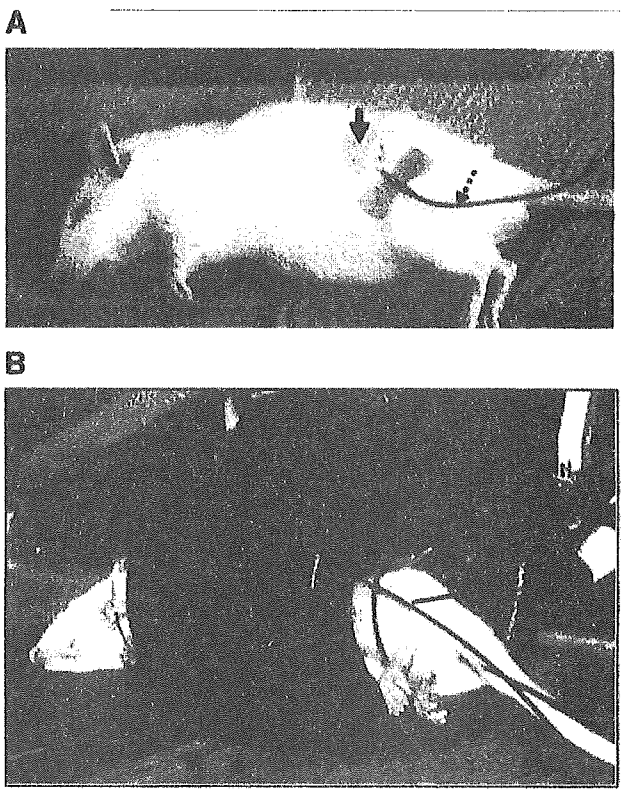

Fig. 2. **A**: Appearance of injection of MCLs with a 26-G syringe needle longitudinally into each prostate cancer nodule subcutaneously from the nodule edge. Solid arrow needle containing MCLs. **B**: Appearance of MCL-induced hyperthermia during exposure to an alternating magnetic field (AMF). The rat was placed inside the horizontal coil (**a**) such that the nodule was positioned at the center of the coil. Optical fiber probes were used to monitor the temperatures at the center of the tumor (**b**) and inside rectum (**c**).

Dai-ichi High Frequency, Tokyo) operating at 118 kHz. The magnetic field intensity was 30.6 kA/m (384 Oe). The rat was placed inside the coil such that the nodule was positioned at the center of the coil (Fig. 2B). Temperatures at the center of the tumor and inside the rectum (representative of the rat body temperature) during AMF were measured by optical fiber probes (FX-9020; Anritsu Meter, Tokyo). The temperature at the center of the tumor was maintained at around 45°C by controlling the magnetic field intensity.

Preparation of Specimens for Immunohistochemical Staining

On the 30th day after the MCL injection, tumors of the two groups were removed and specimens for immunohistochemical staining were prepared as follows. Blood was flushed out with phosphate buffer, then the tumor tissues were extracted, and fixed with Tissue-Tek OCT compound (Sakura Finetechnical, Tokyo) at −20°C. The frozen tumor tissues were sectioned at 10 μm. Tissue sections were air dried for 30 min and fixed with cold acetone for 15 min. These sections were incubated with 5% normal goat serum and 1% skim milk at 37°C for 30 min to block background staining. They were then incubated at 37°C for 60 min with mouse antirat CD3 (1F4), antirat CD4 (W3/25), antirat CD8 (MRC OX-8) monoclonal antibodies (Serotec, Oxford, UK), and antirat HSP70 (W27) monoclonal antibody (Santa Cruz Biotechnology, Santa Cruz, CA) at a dilution of 1:200, and at 37°C for 60 min with goat antimouse monoclonal antibody-conjugated horseradish peroxidase (Caltag Laboratories, Burlingame, CA) at a dilution of 1:200. Each step was followed by washing with the phosphate buffer. Peroxidase activity was visualized by treatment at room temperature for 10 min with 0.02% diaminobenzidine tetrahydrochloride solution containing 0.005% hydrogen peroxidase. All sections were also stained with hematoxylin.

In Vitro Cytotoxicity Assay

Spleen cells were derived from the Group II rats at 1 month after the hyperthermic treatment using the Medimachine System (DAKO, Glostrup, Denmark). Naive rats that had been born at a similar time to the Group II rats were used as the controls. The spleen cells were cultured for 48 hr in RPMI 1640 supplemented with 10% fetal bovine serum and 2-mercaptoethanol ($5 \times 10-5M$). Mouse recombinant interleukin-2 was added once at a concentration of 5 U/ml. The cytotoxicity of spleen cells to prostate cancer cells was determined by a long-term cytotoxicity assay [29]. Rat prostate cancer cells (PLS 10, 1×105 cells) were cultured in a 24-well flat plate containing DMEM. After 24 hr, the medium was replaced with RPMI 1640. Spleen cells were added to each well. The wells were washed with phosphate buffer after 48 hr of incubation at 37°C in an atmosphere containing 5% CO_2. After incubation, 0.3 ml of RPMI 1640 and 0.03 ml of cell-counting solution (kit-8; Dojindo, Kumamoto, Japan) were added to the wells and the cells were incubated for 1 hr at 37°C in an atmosphere containing 5% CO_2. The absorbance of each well was measured at 405 nm with a spectrophotometer (V-530; Jasco, Tokyo). Cytotoxicity was calculated using the following equation: cytotoxicity (%) = [1 − (absorbance of target cells treated with effector cells)/(absorbance of target cells only)] × 100.

Statistical Analysis

Levels of statistical significance in the tumor-growth experiments were evaluated using the Mann–Whitney rank sum test.

RESULTS

Heat Generation by MCLs in AMF

Figure 3 shows the temperature increases at the center of the tumor and inside the rectum of the rats during application of an AMF for 30 min. The temperature at the center of the tumor reached 45°C within 5 min, and was maintained at this temperature by controlling the magnetic field intensity. In contrast, the temperature inside the rectum remained below 38°C. It is noticeable that the temperature at the center of the tumor was maintained very accurately (with a small standard deviation; also for the rectal temperatures),

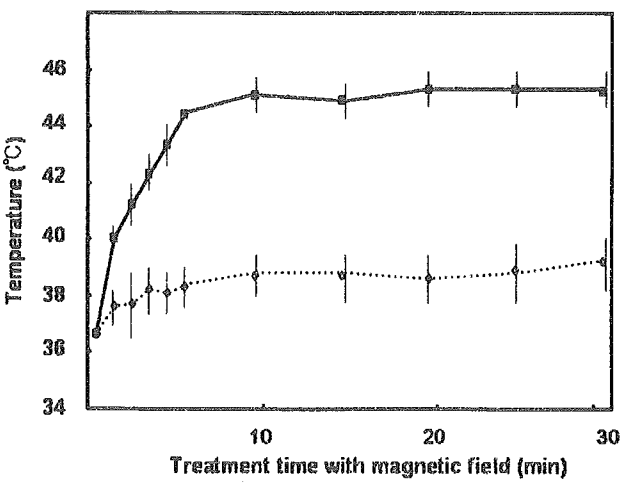

Fig. 3. Temperature increases at the center of the tumor (solid line), and after 10 min is maintained at around 45°C. Temperature inside the rectum (dotted line) increased a little but remained at around 38°C. Values shown are the mean ± SD of five independent experiments.

whereas the temperature difference between the center of the tumor and the rectum was very large (Fig. 3), These results demonstrate that hyperthermia using MCLs makes it feasible to heat only the tumor whilst not damaging healthy tissues.

Monitoring Tumor Growth After Hyperthermia

Figure 4 shows the time course of the tumor-volume growth in five rats in each group. Hyperthermia was induced once the rat prostate cancer nodules had grown to 5–6 mm in diameter. In all rats of Group I (control group), the tumor volume increased linearly. In all rats of Group II (hyperthermic treatment group), the tumor volume increased linearly for 12 days and then was suppressed from days 15 to 21 (and was significantly smaller than that of Group I), after which it did not increase further.

Immunohistological Features of Tumors After Hyperthermic Treatment

To examine whether immunocytes were present in tumor tissue, the tissues of rats with and without hyperthermic treatment were stained immunohistochemically. CD3-, CD4-, and CD8-positive lymphocytes were detected in the tumor tissues of the rats exposed to hyperthermia, but they were not detected in any of the tumor tissue of untreated rats (Fig. 5). HSP 70 was expressed in viable tissue at its boundary with necrotic areas (Fig. 6).

In Vitro Immune Response Using Spleen Cells From Rats Cured by Hyperthermic Treatment

To examine further the mechanisms underlying the antitumor activity of the hyperthermic treatment, we evaluated its effect on the generation of cytotoxic T lymphocyte (CTL)-killing PLS 10 cells. As shown in Figure 7, the CTL activity for PLS 10 cells was approximately twofold higher in spleen cells of Group II rats than in those of naive rats.

DISCUSSION

Hyperthermia treatment is divided into two methods, regional and systemic, with the former being generally selected. Heating methods of regional hyperthermia are divided into external and internal heating. Capacitive hyperthermia with radiofrequency (RF) irradiation is the most common clinical technique, and this represents a type of external, regional hyperthermia treatment. However, RF capacitive hyperthermia is associated with the complication of raising the

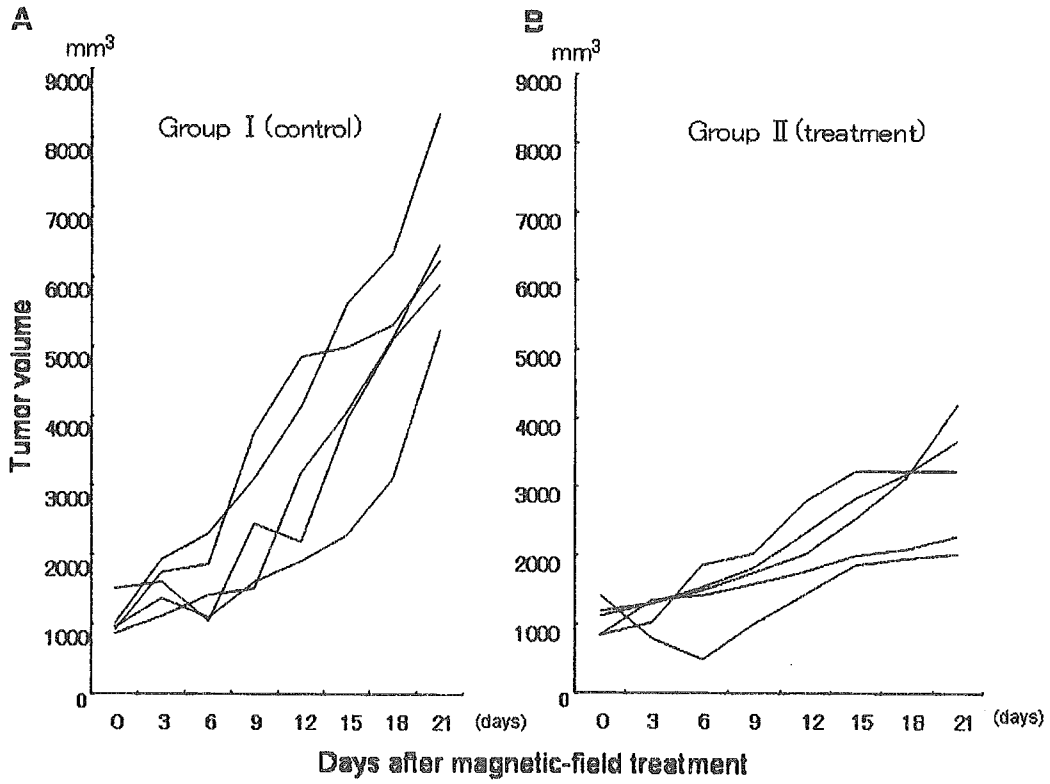

Fig. 4. Time course of tumor-volume growth in each group of five rats: Group I, no treatment (control); Group II, treatment with the AMF. In Group I, the tumor volume increased steadily. In Group II, the growth of all the tumors was suppressed after 15 days.

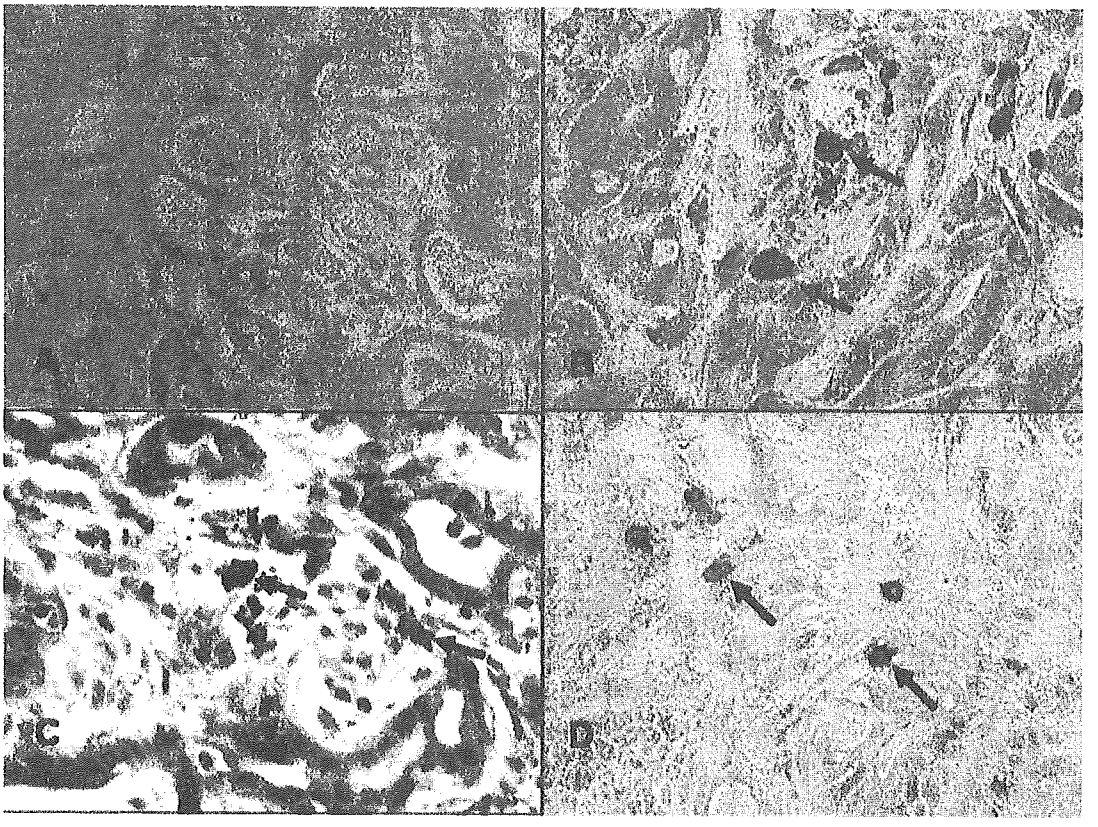

Fig. 5. Immunohistochemical staining for immunocytes. **A**: Tumor tissue of a rat of Group I (control, ×400); no immunocytes appeared. **B, C, D**: Each solid arrows indicates CD3 (B), CD4 (C), and CD8 (D) immunocytes around viable cancer tissue but not necrotic tissue (×400). [Color figure can be viewed in the online issue, which is available at www.interscience.wiley.com.]

body temperature which exerts a massive burden on the patient—it is difficult to heat a tumor specifically with a capacitive heating method using an RF electric field. Kroeze et al. [30] used modeling of capacitive hyperthermia of the prostate to reveal the difficulty of heating deep-seated tumors in the pelvic area. We have developed MCLs for implementing intracellular hyperthermia in vivo without the disadvantage of

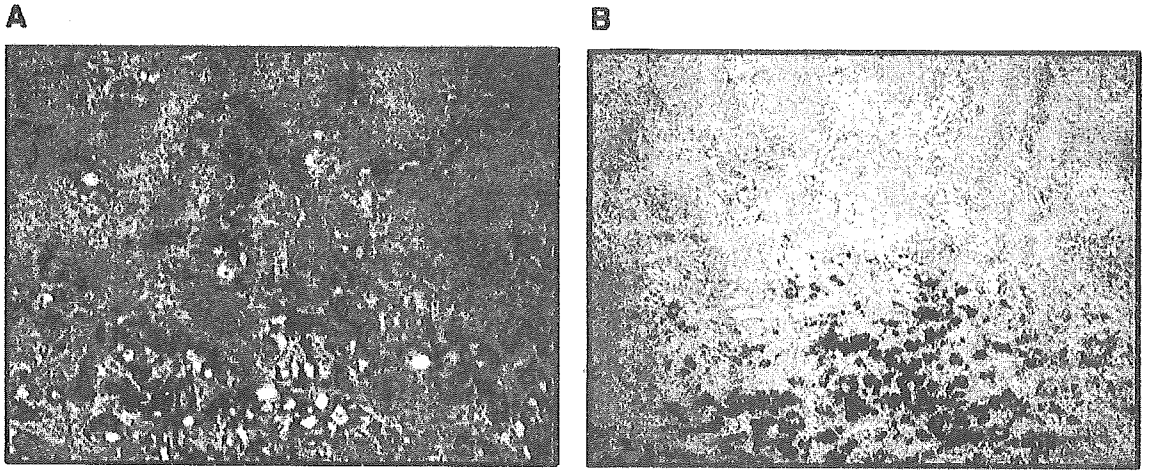

Fig. 6. **A**: Histology of tumor tissue for a rat of Group II. Necrotic tissue was present at the specimen center (*), and viable cancer tissue was present around the necrotic tissue (**). H-E stain, ×200. **B**: Light-microscopy section of anti-HSP70 antibody staining at the boundary between necrotic and viable areas at the same position of A. HSP70 appeared in the viable area but not in the necrotic area. [Color figure can be viewed in the online issue, which is available at www.interscience.wiley.com.]

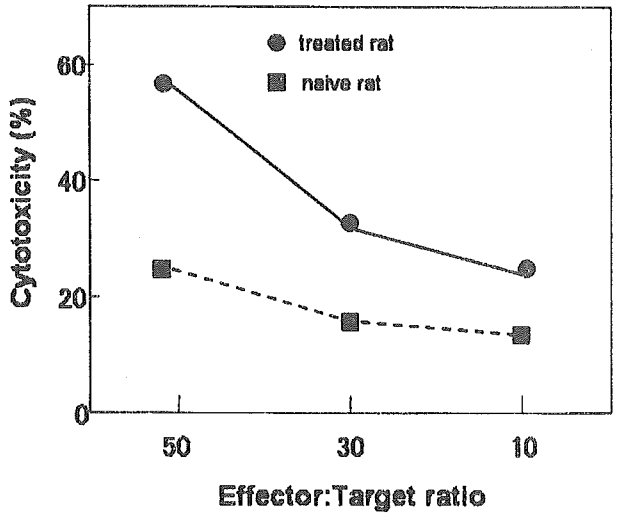

Fig. 7. Activity of antitumor cytotoxic T lymphocytes (CTLs) in rats that had been suppressed by the hyperthermic treatment. ●: The CTL activity for PLS 10 cells from spleen cells of treated rats. ■: The CTL activity of spleen cells of naive rats for PLS 10 cells.

RF capacitive hyperthermia [23,24]. According to the criteria of hyperthermia, our hyperthermia method using MCLs in an AMF (MCL-induced hyperthermia) represents a type of internal, regional hyperthermia treatment. For the purpose of applying MCL-induced hyperthermia to the future clinical treatment of patients with prostate cancer, in the present study this technique was applied to rat prostate cancer in vivo. This study investigated the following four factors: (1) whether the temperature of rat prostate cancer nodules increases, (2) whether body temperature also increases, (3) the effect on rat prostate cancer regression, and (4) the presence of mechanisms other than heating. In this experiment, prostate cancer derived from the prostate of F344 rats are transplanted into syngeneic rats, which differs significantly from the experiment in which human tumor tissue is transplanted into nude mice. This experiment therefore represents an excellent model for evaluating host immune responses to tumor tissue.

In this study, the temperature at the center of the tumor reached 45°C within 5 min, and was maintained for 20 min at this level by controlling the magnetic field intensity. In contrast, the temperature inside the rectum, which is representative rat body temperature, remained below 38°C. These results demonstrate that MCL-induced hyperthermia is able to increase the tumor temperature whilst not also increasing the overall body temperature.

The tumor-volume growth rate demonstrated that the growth of prostate cancer nodules was clearly suppressed by the heating of MCLs with an AMF. However, the prostate cancer nodules did not disappear completely under the present experimental conditions. This is the first examination of MCL-induced hyperthermia for rat prostate cancer and hence the injection of an adequate amount of MCLs into the optimal position for prostate cancer would make it possible to cure prostate cancer by heating with AMF. And one of the significant points of our MCL-induced hyperthermia method is specific MCLs injection to tumor tissue. It is difficult to inject MCLs into lesions that are located deep in the body or lesions with hypervascularity such as in hepatic cancer and renal tumors. However, the technique of injection of MCLs can be readily applied to the treatment of prostate cancer. Three-dimensional computerized tomography or transrectal ultrasound techniques, as used to guide interstitial brachytherapy for prostate cancer [31–33], could also be applied for the accurate injection of MCLs to tumor tissue.

In addition to heating, our MCL-induced hyperthermia technique is suggested to induce an immune response. In this study, CD3-, CD4-, and CD8-positive lymphocytes appeared around the border between necrotic tissue and viable tumor tissue. CD4 cells recognize antigen-presenting cells (such as macrophages) which, when activated, play roles in the activation of B cells to antibody-producing cells and in the activation of CD8 cells to CTLs. On the other hand, CD8 cells recognize antigen-bearing cells such as virus-infected cells and tumor cells, and themselves change into CTLs. Both cell types were observed in the present study, suggesting that CD8 cells were activated to CTLs by CD4 cells. Our results clearly demonstrate that antitumor T lymphocytes were amplified by the induction of hyperthermia, and that this amplification would lead to destruction of the tumor. Both CD8 and CD4 T lymphocytes were detected in the tumor tissue of rats subjected to the hyperthermic treatment, while no immunocytes was observed in untreated rats. These results suggest that activation of T lymphocytes at the tumor site after hyperthermia is attributable to tissue necrosis.

In contrast, HSP70 also appeared in viable tissue at its boundary with necrotic tissue. Hyperthermia is known to induce HSPs [34]. Until now, the expression of HSPs was considered an unwanted side effect of hyperthermia because HSPs cause thermotolerance in tumor tissue [35]. However, HSP-mediated antitumor immunity was reported to cause a vaccine effect of HSP-peptide complexes released from tumor cells [36–38]. Blom et al. [39] reported that the expression of HSP70 was increased after exposure of melanoma cells to a temperature of 45°C. Our MCL-induced hyperthermia also induced HSP70 in a viable area of tumor tissue. The progression of T lymphocytes was also caused by the

elevated expression of HSPs, which is characteristic of heat treatment [40,41].

A CTL assay was therefore used to investigate the in vivo immune response of rats after MCL-included hyperthermia, and an approximately twofold higher activity of CTL was induced in spleen cells. These data demonstrate that the immune response was induced specifically in PLS 10 cells and that even if viable cells remain in a tumor after hyperthermia, they will become targets for the antitumor immune reaction and complete tumor regression may eventually occur.

The present study shows that our MCL-induced hyperthermia technique is an effective therapy for the treatment of prostate cancer, since this treatment kills tumor cells not only directly by heating but also by inducing an immune response. That the new technique described here represents an epoch-making therapy having the possibility to treat both primary and metastatic tumors.

There are many problems that should be resolved before the application of our MCL-induced hyperthermia technique to clinical cases. These include the development of an AMF irradiation device suitable for the human body and a safety investigation of the use of MCLs in the human body. The injection of MCLs into tumor tissue, however, is made easier with the assistance of three-dimensional computerized tomography or transrectal ultrasound techniques. MCL-induced hyperthermia therefore does not have the disadvantage associated with RF hyperthermia. Moreover, by inducing an immune response, our technique opens the possibility of treating both primary and metastatic lesions, and hence should be considered a useful future therapy for prostate cancer.

REFERENCES

1. Levi F, Lucchini F, Negri E, Boyle P, La Vecchia C. Changed trends of cancer mortality in the elderly. Ann Oncol 2001;12: 1467–1477.
2. Littrup PJ. Future benefits and cost-effectiveness of prostate carcinoma screening. American Cancer Society. Cancer 1997;80: 1864–1870.
3. Smart CR. The results of prostate carcinoma screening in the US as reflected in the surveillance, epidemiology, and end results program. Cancer 1997;80:1835–1844.
4. Schellhammer PF. Editorial: Improving outcomes for primary and salvage therapy of localized prostate cancer. J Urol 2003;170: 1841–1842.
5. Akaza H, Homma Y, Okada K, Yokoyama M, Moriyama N, Usami M, Hirao Y, Tsushima T, Ohashi Y, Aso Y. Early results of LH-RH agonist treatment with or without chlormadinone acetate for hormone therapy of naive localized or locally advanced prostate cancer: A prospective and randomized study. The Prostate Cancer Study Group. Jpn J Clin Oncol 2000;30:131–136.
6. Han KR, Cohen JK, Miller RJ, Pantuck AJ, Freitas DG, Cuevas CA, Kim HL, Lugg J, Childs SJ, Shuman B, Jayson MA, Shore ND, Moore Y, Zisman A, Lee JY, Ugarte R, Mynderse LA, Wilson TM, Sweat SD, Zincke H, Belldegrun AS. Treatment of organ confined prostate cancer with third generation cryosurgery: Preliminary multicenter experience. J Urol 2003;170:1126–1130.
7. Chin JL, Touma N, Pautler SE, Guram KS, Bella AJ, Downey DB, Moussa M. Serial histopathology results of salvage cryoablation for prostate cancer after radiation failure. J Urol 2003;170:1199–1202.
8. Johnson DB, Nakada SY. Cryoablation of renal and prostate tumors. J Endourol 2003;17:627–632.
9. Rouviere O, Lyonnet D, Radiant A, Colin-Pan gaud C, Chapelon JY, Bouvier R, Dubernard JM, Gelet A. MRI appearance of prostate following transrectal HIFU ablation of localized cancer. Eur Urol 2001;40:265–274.
10. Gelet A, Chapelon JY, Bouvier R, Pangaud C, Lasne Y. Local control of prostate cancer by transrectal high intensity focused ultrasound therapy: Preliminary results. J Urol 1999;161:156–162.
11. Van Leenders GJ, Beerlage HP, Ruijter ET, de la Rosette JJ, van de Kaa CA. Histopathological changes associated with high intensity focused ultrasound (HIFU) treatment for localised adenocarcinoma of the prostate. J Clin Pathol 2000;53:391–394.
12. Ryu S, Brown SL, Kim SH, Khil MS, Kim JH. Preferential radiosensitization of human prostatic carcinoma cells by mild hyperthermia. Int J Radiat Oncol Biol Phys 1996;34:133–138.
13. Hurwitz MD, Kaplan ID, Svensson GK, Hynynen K, Hansen MS. Feasibility and patient tolerance of a novel transrectal ultrasound hyperthermia system for treatment of prostate cancer. Int J Hyperthermia 2001;17:27–31.
14. Algan O, Fosmire H, Hynynen K, Dalkin B, Cui H, Drach G, Stea B, Cassady JR. External beam radiotherapy and hyperthermia in the treatment of patients with locally advanced prostate carcinoma. Cancer 2000;89:399–403.
15. Prionas SD, Kapp DS, Goffinet DR, Ben-Yosef R, Fessenden P, Bagshaw MA. Thermometry of interstitial hyperthermia given as an adjuvant to brachytherapy for the treatment of carcinoma of the prostate. Int J Radiat Oncol Biol Phys 1994;28:151–162.
16. Anscher MS, Samulski TV, Dodge R, Prosnitz LR, Dewhirst MW. Combined external beam irradiation and external regional hyperthermia for locally advanced adenocarcinoma of the prostate. Int J Radiat Oncol Biol Phys 1997;37:1059–1065.
17. Petrovich Z, Emami B, Kapp D, Sapozink MD, Langholz B, Oleson J, Lieskovsky G. Astrahan M. Regional hyperthermia in patients with recurrent genitourinary cancer. Am J Clin Oncol 1991;14:472–477.
18. van Vulpen M, Raaymakers BW, Lagendijk JJ, Crezee J, de Leeuw AA, van Moorselaar JR, Ligtvoet CM, Battermann JJ. Three-dimensional controlled interstitial hyperthermia combined with radiotherapy for locally advanced prostate carcinoma—A feasibility study. Int J Radiat Oncol Biol Phys 2002;53:116–126.
19. Connor WG, Gerner EW, Miller RC, Boone ML. Prospects for hyperthermia in human cancer therapy. Part II: Implications of biological and physical data for applications of hyperthermia to man. Radiology 1977;123:497–503.
20. Jordan A, Wust P, Fahling H, John W, Hinz A, Felix R. Inductive heating of ferrimagnetic particles and magnetic fluids: Physical evaluation of their potential for hyperthermia. Int J Hyperthermia 1993;9:51–68.
21. Mitsumori M, Hiraoka M, Shibata T, Okuno Y, Masunaga S, Koishi M, Okajima K. Nagata Y, Nishimura Y, Abe M. Development of intra-arterial hyperthermia using a dextran-magnetite complex. Int J Hyperthermia 1994;10:785–793.

22. Shinkai M, Matsui M, Kobayashi T. Heat properties of magnetoliposomes for local hyperthermia. Jpn J Hyperthermic Oncol 1994;10:168–177.
23. Shinkai M, Yanase M, Honda H, Wakabayashi T, Yoshida J, Kobayashi T. Intracellular hyperthermia for cancer using magnetite cationic liposomes: In vitro study. Jpn J Cancer Res 1996;87:1179–1183.
24. Yanase M, Shinkai M, Honda H, Wakabayashi T, Yoshida J, Kobayashi T. Intracellular hyperthermia for cancer using magnetite cationic liposomes: Ex vivo study. Jpn J Cancer Res 1997;88:630–632.
25. Yanase M, Shinkai M, Honda H, Wakabayashi T, Yoshida J, Kobayashi T. Intracellular hyperthermia for cancer using magnetite cationic liposomes: An in vivo study. Jpn J Cancer Res 1998;89:463–469.
26. Yanase M, Shinkai M, Honda H, Wakabayashi T, Yoshida J, Kobayashi T. Antitumor immunity induction by intracellular hyperthermia using magnetite cationic liposomes. Jpn J Cancer Res 1998;89:775–782.
27. Nakanishi H, Takeuchi S, Kato K, Shimizu S, Kobayashi K, Tatematsu M, Shirai T. Establishment and characterization of three androgen-independent, metastatic carcinoma cell lines from 3,2′-dimethyl-4-aminobiphenyl-induced prostatic tumors in F344 rats. Jpn J Cancer Res 1996;87:1218–1226.
28. Owen CS, Sykes NL. Magnetic labeling and cell sorting. J Immunol Methods 1984;73:41–48.
29. Aruga A, Aruga E, Chang AE. Reduced efficacy of allogeneic versus syngeneic fibroblasts modified to secrete cytokines as a tumor vaccine adjuvant. Cancer Res 1997;57:3230–3237.
30. Kroeze H, Van de Kamer JB, De Leeuw AA, Lagendijk JJ. Regional hyperthermia applicator design using FDTD modeling. Phys Med Biol 2001;46:1919–1935.
31. Wang H, Wallner K, Sutlief S, Blasko J, Russell K, Ellis W. Transperineal brachytherapy in patients with large prostate glands. Int J Cancer 2000;90:199–205.
32. Merrick GS, Wallner KE, Butler WM. Permanent interstitial brachytherapy for the management of carcinoma of the prostate gland. J Urol 2003;169:1643–1652.
33. Koutrouvelis PG, Lailas N, Katz S, Sehn J, Gil-Montero G, Khawand N. Prostate cancer with large glands treated with 3-dimensional computerized tomography guided pararectal brachytherapy: Up to 8 years of followup. J Urol 2003;169: 1331–1336.
34. Burdon RH, Slater A, McMahon M, Cato AC. Hyperthermia and the heat-shock proteins of HeLa cells. Br J Cancer 1982;45: 953–963.
35. Sciandra JJ, Subjeck JR. Heat shock proteins and protection of proliferation and translation in mammalian cells. Cancer Res 1984;44:5188–5194.
36. Castelli C, Ciupitu AM, Rini F, Rivoltini L, Mazzocchi A, Kiessling R, Parmiani G. Human heat shock protein 70 peptide complexes specifically activate antimelanoma T cells. Cancer Res 2001;61:222–227.
37. Ito A, Shinkai M, Honda H, Yoshikawa K, Saga S, Wakabayashi T, Yoshida J, Kobayashi T. Heat shock protein 70 expression induces antitumor immunity during intracellular hyperthermia using magnetite nanoparticles. Cancer Immunol Immunother 2003;52:80–83.
38. Huang C, Yu H, Wang Q, Ma W, Xia D, Yi P, Zhang L, Cao X. Potent antitumor effect elicited by superantigen-linked tumor cells transduced with heat shock protein 70 gene. Cancer Sci 2004;95:160–167.
39. Blom DJ, De Waard-Siebinga I, Apte RS, Luyten GP, Niederkorn JY, Jager MJ. Effect of hyperthermia on expression of histocompatibility antigens and heat-shock protein molecules on three human ocular melanoma cell lines. Melanoma Res 1997;7:103–109.
40. Kobayashi N, Matsuzaki G, Yoshikai Y, Seki R, Ivanyi J, Nomoto K. V delta 5+ T cells of BALB/c mice recognize the murine heat shock protein 60 target cell specificity. Immunology 1994;81:240–246.
41. Ueda G, Tamura Y, Hirai I, Kamiguchi K, Ichimiya S, Torigoe T, Hiratsuka H, Sunakawa H, Sato N. Tumor-derived heat shock protein 70-pulsed dendritic cells elicit tumor-specific cytotoxic T lymphocytes (CTLs) and tumor immunity. Cancer Sci 2004;95: 248–253.

Pilot study of combined dermoscopy and reflectance confocal microscopy evaluation for the early detection of basal cell carcinoma

Jiro Ogino, MD, Toshiharu Yamashita, MD, PhD, Ichiro Ono, MD, PhD, Akiko Sakemoto, MD, Takafumi Kamiya, MD, Rie Kaneko, MD, Kuninori Hirosaki, MD, PhD, Kenji Saga, MD, PhD, and Kowichi Jimbow, MD, PhD, FRCPC

Department of Dermatology, Sapporo Medical University School of Medicine, Sapporo, Japan

Correspondence and reprint requests:

Kowichi Jimbow MD, PhD, FRCPC

Department of Dermatology, Sapporo Medical University School of Medicine

Chuo-ku, Minami 1, Nishi 16, Sapporo, Japan

Phone: 81-11-611-2111 Fax: 81-11-613-3739 E-mail: jimbow@sapmed.ac.jp

Text word: 998 words, references: 13, tables: 1, figures: 2

Running head: RCM detection of early/micro BCC

This study was supported in part by Grants-in-Aid from the Ministry of Education, Sports and Culture of Japan, and Ministry of Health, Labour and Welfare of Health and Labour Sciences Research Grants of Research on Advanced Medical Technology. A part of this study is also supported by Stiefel Inc.